Supporting Material - Long-term changes in the timing and intensity of the pollen season in Slovenia (2002 – 2024)

Rene Markovič[1,2*], Vladimir Grubelnik[2], Anja Simčič[3], Andreja Kofol Seliger[3], Urška Razboršek[3], Marko Marhl[1,4,5], Uroš Lešnik[3]

1 Faculty of Natural Sciences and Mathematics, University of Maribor, Koroška cesta 160, SI-2000 Maribor, Slovenia

2 Faculty of Electrical Engineering and Computer Science, University of Maribor, Koroška cesta 46, 2000, Maribor, Slovenia

3 National Laboratory of Health, Environment and Food, Prvomajska ulica 1, SI-2000 Maribor, Slovenia

4 Faculty of Education, University of Maribor, Koroška cesta 160, 2000, Maribor, Slovenia

5 Faculty of Medicine, University of Maribor, Taborska ulica 8, 2000, Maribor, Slovenia

* Correspondence to: Rene Markovič Faculty of Natural Sciences and Mathematics, University of Maribor Koroška cesta 160, SI-2000 Maribor, Slovenia

Email: rene.markovic@um.si

Phone: +386 2 220 73 91

This document contains comprehensive visual analysis results for pollen data across three regions: Ljubljana, Maribor, and Primorje, along with cross-regional correlation analyses.

Pripombe dodal [UR1]: Primorje je bilo nekajkrat pisano z malo - smo popravili po celotnem besedilu

Ljubljana Analysis Results

This section contains all analysis results for Ljubljana, including global overviews, data completeness assessments, statistical analyses, and type-specific results.

Global Overview Analysis

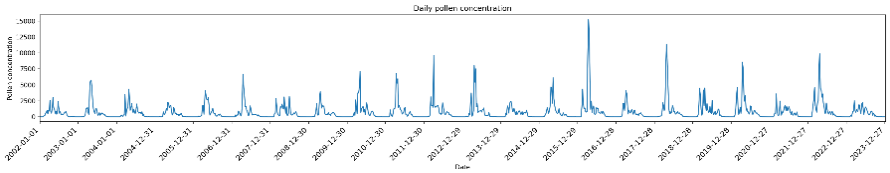

Figure S1a: Global Overview Analysis of Pollen in Ljubljana, Slovenia, highlighting the seasonal distribution and abundance of various pollen species in the region.

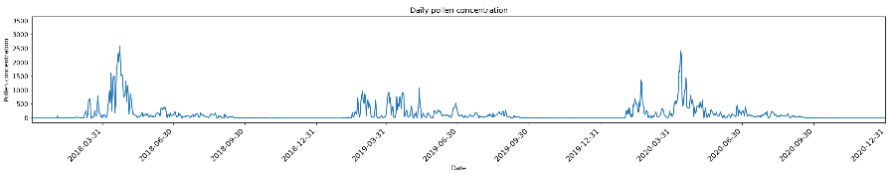

Figure S1b: Global overview pollen diagram for Ljubljana, Slovenia, illustrating the seasonal patterns of major tree and grass pollen species in the region.

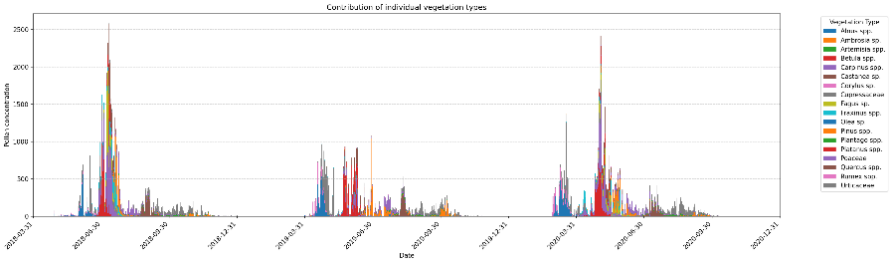

Figure S1c: Global overview of pollen records from Ljubljana, Slovenia, highlighting seasonal patterns and species distribution across the region.

Data Completeness Assessment

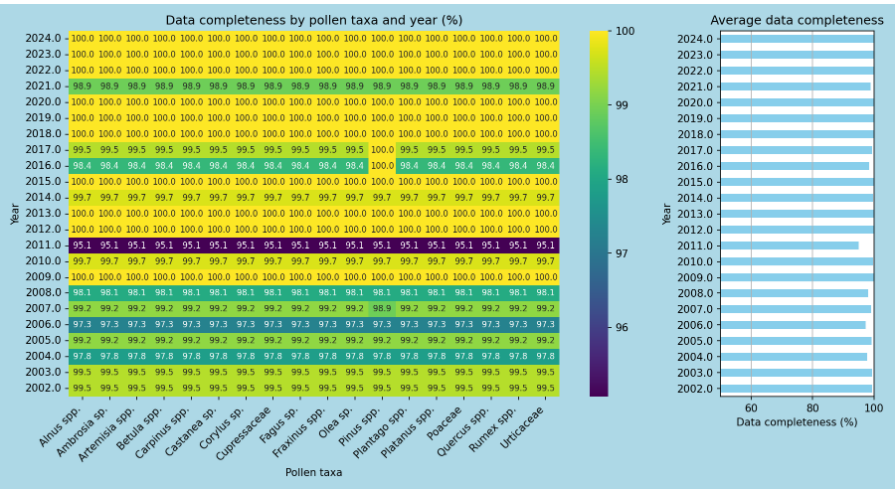

Figure S2a: Annual pollen data completeness assessment for Ljubljana, Slovenia, showing the percentage of pollen samples collected and analyzed each month over a one-year period.

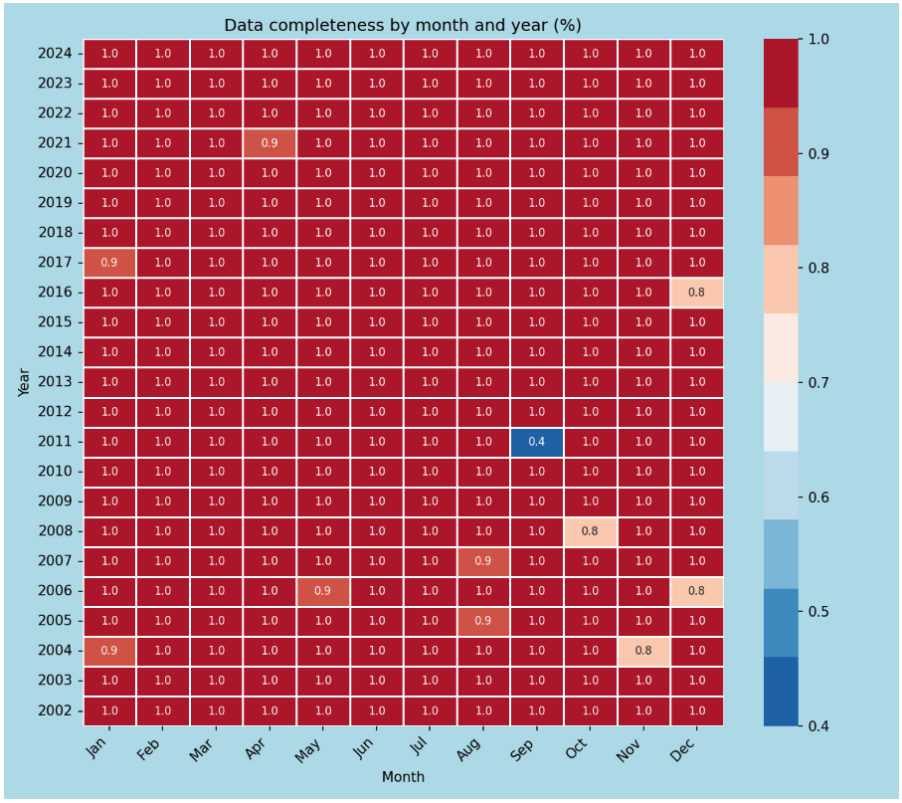

Figure S2b: Monthly pollen data completeness assessment for Ljubljana, Slovenia. The figure displays the proportion of dataset completeness for individual months of a given year. The color-bar on the right displays the color mapping of completeness values, where red indicates complete data (1.0 or 100%), and lighter shades represent incomplete data, with blue indicating the lowest completeness values (0.4 or 40%). Each cell shows the completeness proportion for a specific month-year combination, revealing that most months have complete data (1.0).

Season statistics for Ljubljana, Slovenia

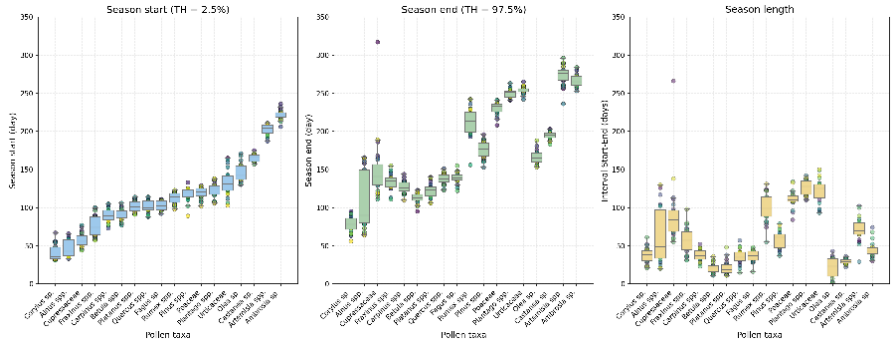

Figure S3: Pollen season metrics across taxa in Ljubljana, Slovenia. Box plots showing (left) season start day expressed as day of year using the 2.5% threshold of cumulative annual pollen count, (middle) season end day using the 97.5% threshold, and (right) season length in days calculated as the difference between season end and start dates. Each box represents the interquartile range (IQR) with the median shown as a horizontal line, whiskers extend to 1.5×IQR, and outliers are shown as individual points. Pollen taxa are ordered chronologically based on their typical season timing, with early-season taxa (*Corylus*, *Alnus*) on the left and late-season taxa (*Artemisia*, *Ambrosia*) on the right.

Pripombe dodal [UR2]: Nekateri taksoni v besedilu niso bili napisani poševno. Vse take smo popravili.

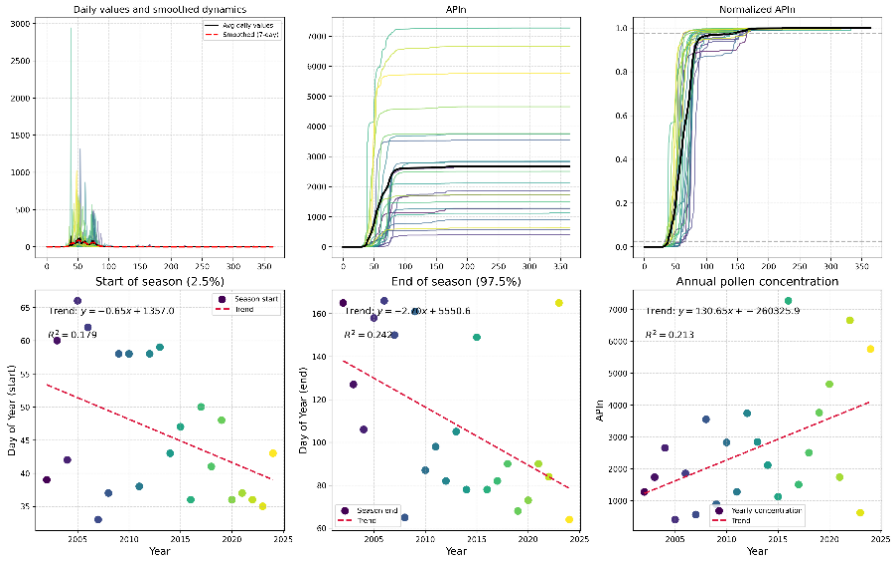

Figure S4a: Example of the pollen season analysis pipeline applied to *Alnus* spp. (alder) in Ljubljana. The top row presents the seasonal dynamics and data normalization: (upper left) daily pollen concentrations showing average values (black line) and 7-day smoothing (red dashed line); (upper middle) cumulative annual pollen totals; and (upper right) normalized cumulative sums used for phenological thresholding. The bottom row illustrates inter-annual trends over the 23-year period (2002-2024) for (lower left) season start day (2.5% threshold), (lower middle) season end day (97.5% threshold), and (lower right) the annual pollen integral (APIn). Linear regression lines and coefficients of determination (R^2) highlight a shift toward an earlier and more intense pollen season.

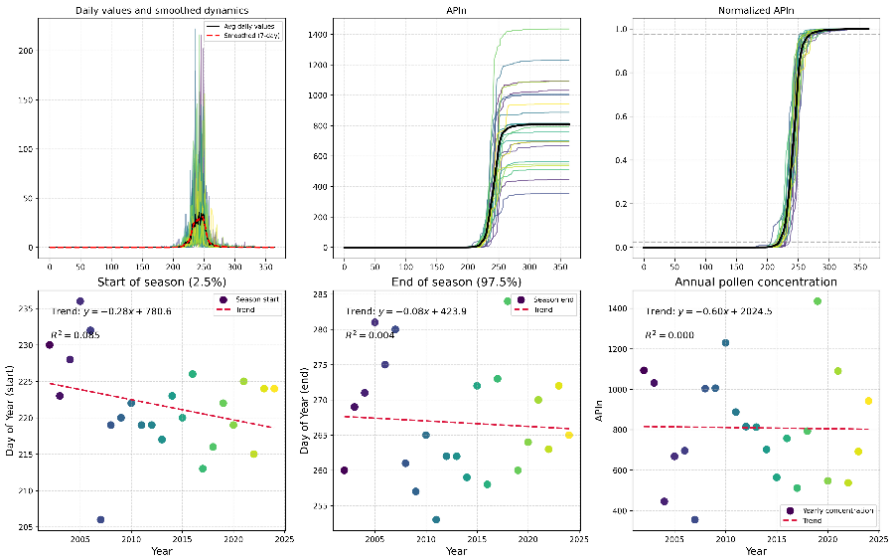

Figure S4b: Example of the pollen season analysis pipeline applied to *Ambrosia* sp. (ragweed) in Ljubljana. The top row presents the seasonal dynamics and data normalization: (upper left) daily pollen concentrations showing average values (black line) and 7-day smoothing (red dashed line); (upper middle) cumulative annual pollen totals; and (upper right) normalized cumulative sums used for phenological thresholding. The bottom row illustrates inter-annual trends over the 23-year period (2002-2024) for (lower left) season start day (2.5% threshold), (lower middle) season end day (97.5% threshold), and (lower right) the annual pollen integral (APIn). Linear regression lines and coefficients of determination (R^2) highlight a shift toward an earlier and more intense pollen season.

Pripombe dodal [UR3]: Kjer ni bilo angleškega imena taksona smo ga dopisali

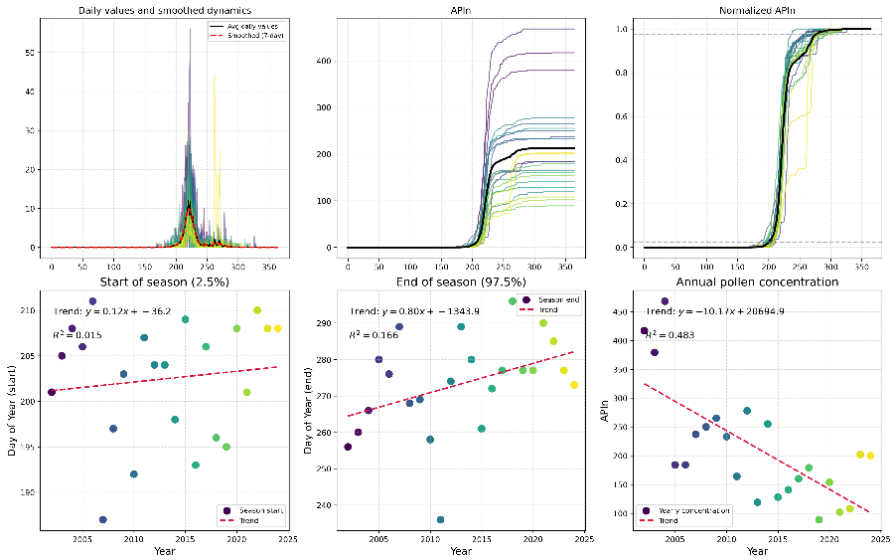

Figure S4c: Example of the pollen season analysis pipeline applied to *Artemisia* spp. (mugwort) in Ljubljana. The top row presents the seasonal dynamics and data normalization: (upper left) daily pollen concentrations showing average values (black line) and 7-day smoothing (red dashed line); (upper middle) cumulative annual pollen totals; and (upper right) normalized cumulative sums used for phenological thresholding. The bottom row illustrates inter-annual trends over the 23-year period (2002-2024) for (lower left) season start day (2.5% threshold), (lower middle) season end day (97.5% threshold), and (lower right) the annual pollen integral (APIn). Linear regression lines and coefficients of determination (R^2) highlight a shift toward an earlier and more intense pollen season.

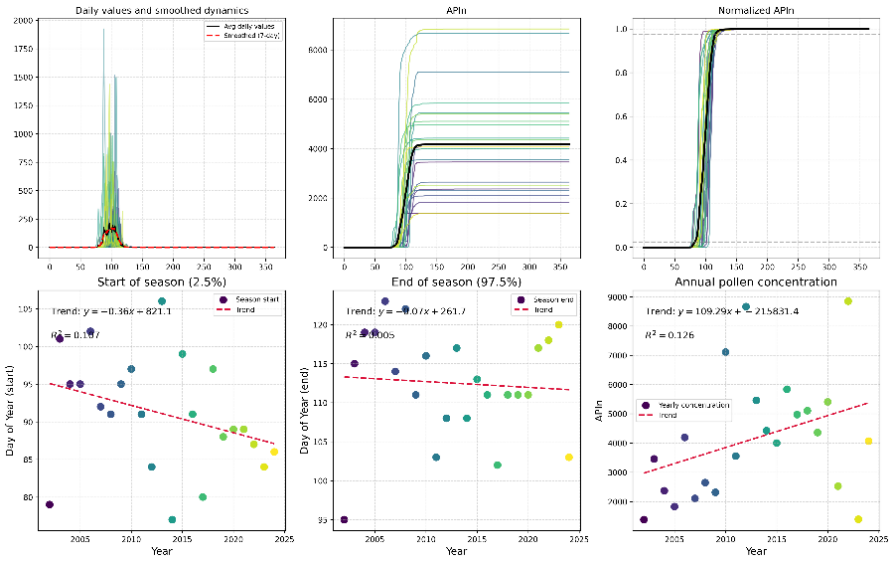

Figure S4d: Example of the pollen season analysis pipeline applied to *Betula* spp. (birch) in Ljubljana. The top row presents the seasonal dynamics and data normalization: (upper left) daily pollen concentrations showing average values (black line) and 7-day smoothing (red dashed line); (upper middle) cumulative annual pollen totals; and (upper right) normalized cumulative sums used for phenological thresholding. The bottom row illustrates inter-annual trends over the 23-year period (2002-2024) for (lower left) season start day (2.5% threshold), (lower middle) season end day (97.5% threshold), and (lower right) the annual pollen integral (APIn). Linear regression lines and coefficients of determination (R^2) highlight a shift toward an earlier and more intense pollen season.

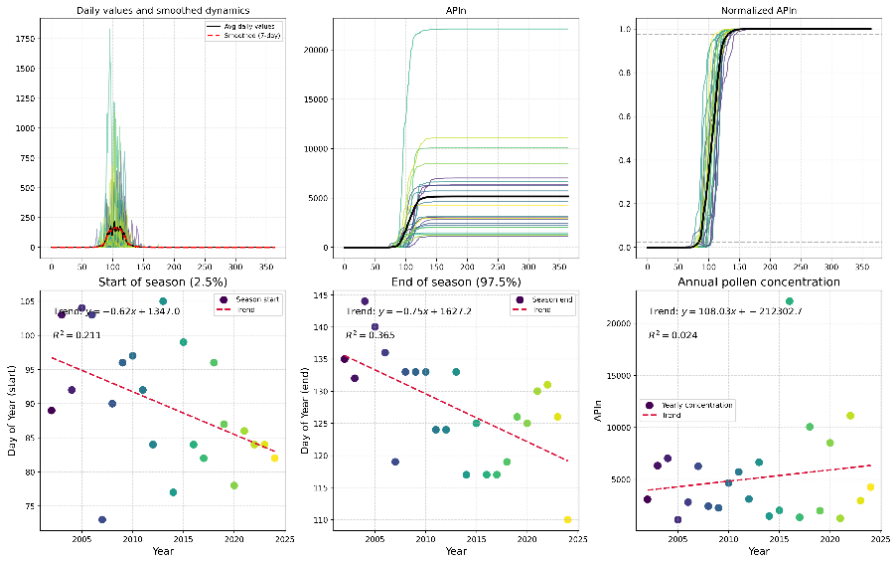

Figure S4e: Example of the pollen season analysis pipeline applied to *Carpinus* spp./*Ostrya* spp. (hornbeam/hop-hornbeam) in Ljubljana. The top row presents the seasonal dynamics and data normalization: (upper left) daily pollen concentrations showing average values (black line) and 7-day smoothing (red dashed line); (upper middle) cumulative annual pollen totals; and (upper right) normalized cumulative sums used for phenological thresholding. The bottom row illustrates inter-annual trends over the 23-year period (2002-2024) for (lower left) season start day (2.5% threshold), (lower middle) season end day (97.5% threshold), and (lower right) the annual pollen integral (APIn). Linear regression lines and coefficients of determination (R^2) highlight a shift toward an earlier and more intense pollen season.

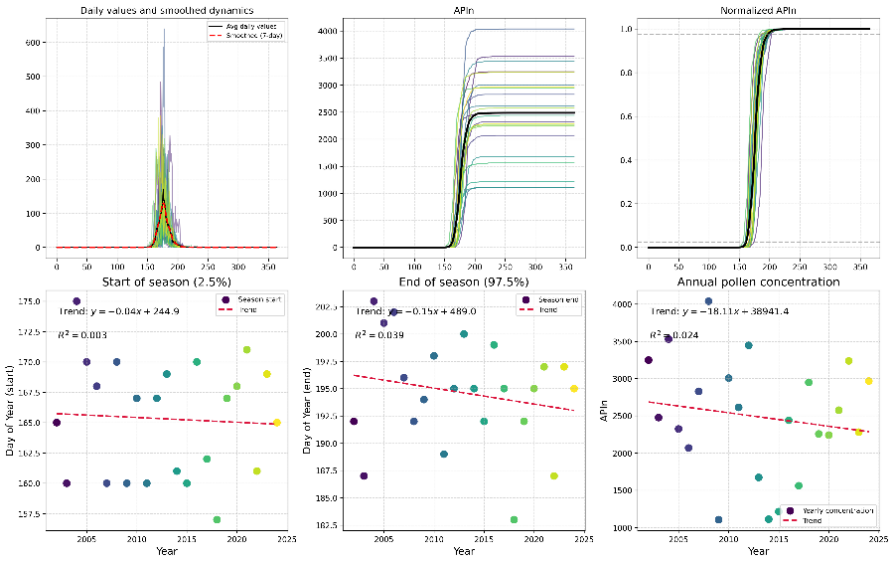

Figure S4f: Example of the pollen season analysis pipeline applied to *Castanea* sp. (sweet chestnut) in Ljubljana. The top row presents the seasonal dynamics and data normalization: (upper left) daily pollen concentrations showing average values (black line) and 7-day smoothing (red dashed line); (upper middle) cumulative annual pollen totals; and (upper right) normalized cumulative sums used for phenological thresholding. The bottom row illustrates inter-annual trends over the 23-year period (2002-2024) for (lower left) season start day (2.5% threshold), (lower middle) season end day (97.5% threshold), and (lower right) the annual pollen integral (APIn). Linear regression lines and coefficients of determination (R^2) highlight a shift toward an earlier and more intense pollen season.

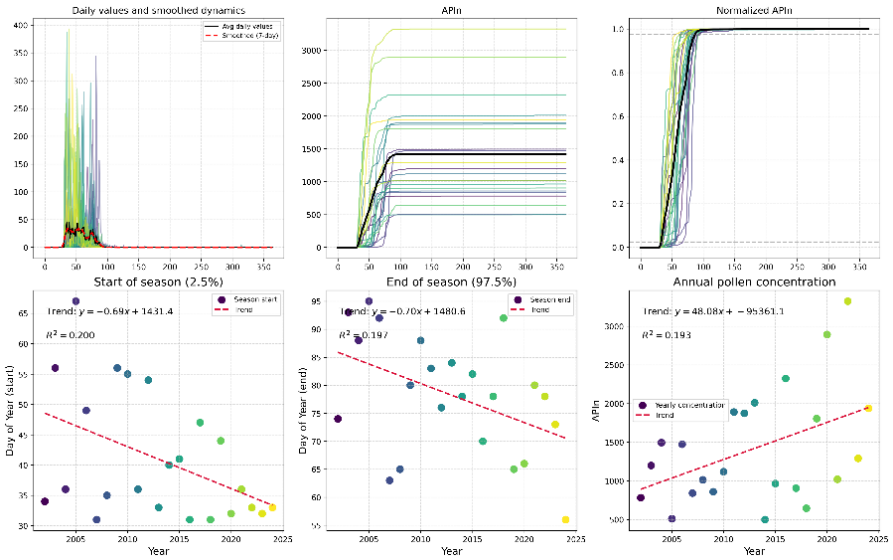

Figure S4g: Example of the pollen season analysis pipeline applied to *Corylus* sp. (hazel) in Ljubljana. The top row presents the seasonal dynamics and data normalization: (upper left) daily pollen concentrations showing average values (black line) and 7-day smoothing (red dashed line); (upper middle) cumulative annual pollen totals; and (upper right) normalized cumulative sums used for phenological thresholding. The bottom row illustrates inter-annual trends over the 23-year period (2002-2024) for (lower left) season start day (2.5% threshold), (lower middle) season end day (97.5% threshold), and (lower right) the annual pollen integral (APIn). Linear regression lines and coefficients of determination (R^2) highlight a shift toward an earlier and more intense pollen season.

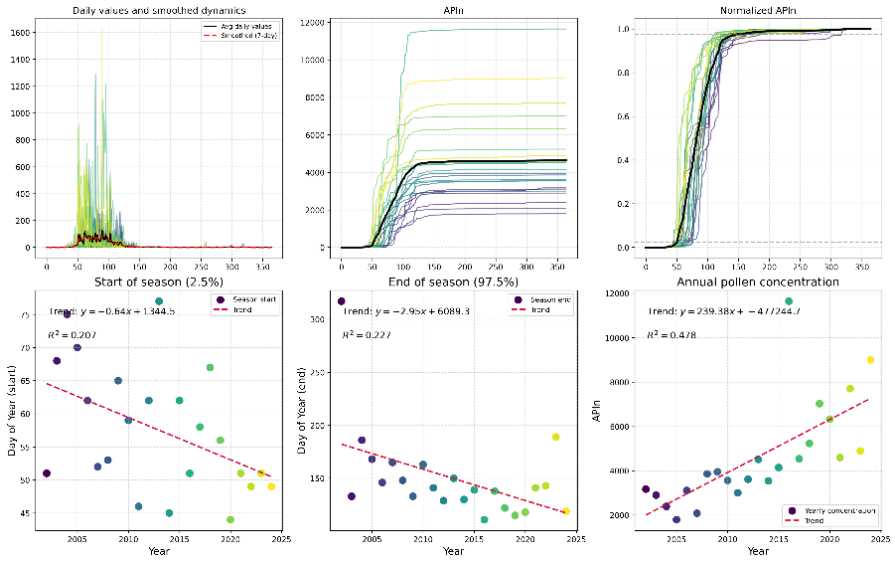

Figure S4h: Example of the pollen season analysis pipeline applied to Cupressaceae/Taxaceae (cypress/yew) in Ljubljana. The top row presents the seasonal dynamics and data normalization: (upper left) daily pollen concentrations showing average values (black line) and 7-day smoothing (red dashed line); (upper middle) cumulative annual pollen totals; and (upper right) normalized cumulative sums used for phenological thresholding. The bottom row illustrates inter-annual trends over the 23-year period (2002-2024) for (lower left) season start day (2.5% threshold), (lower middle) season end day (97.5% threshold), and (lower right) the annual pollen integral (APIn). Linear regression lines and coefficients of determination (R^2) highlight a shift toward an earlier and more intense pollen season.

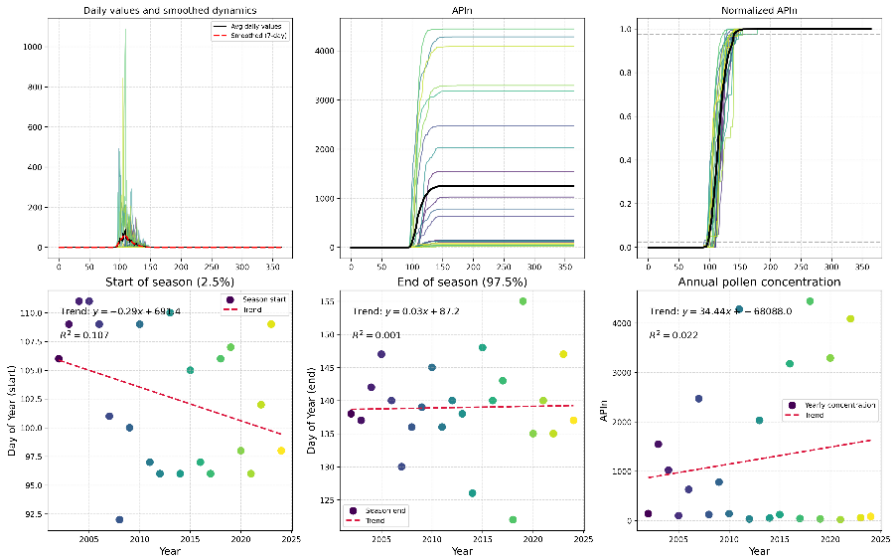

Figure S4i: Example of the pollen season analysis pipeline applied to *Fagus* sp. (beech) in Ljubljana. The top row presents the seasonal dynamics and data normalization: (upper left) daily pollen concentrations showing average values (black line) and 7-day smoothing (red dashed line); (upper middle) cumulative annual pollen totals; and (upper right) normalized cumulative sums used for phenological thresholding. The bottom row illustrates inter-annual trends over the 23-year period (2002-2024) for (lower left) season start day (2.5% threshold), (lower middle) season end day (97.5% threshold), and (lower right) the annual pollen integral (APIn). Linear regression lines and coefficients of determination (R^2) highlight a shift toward an earlier and more intense pollen season.

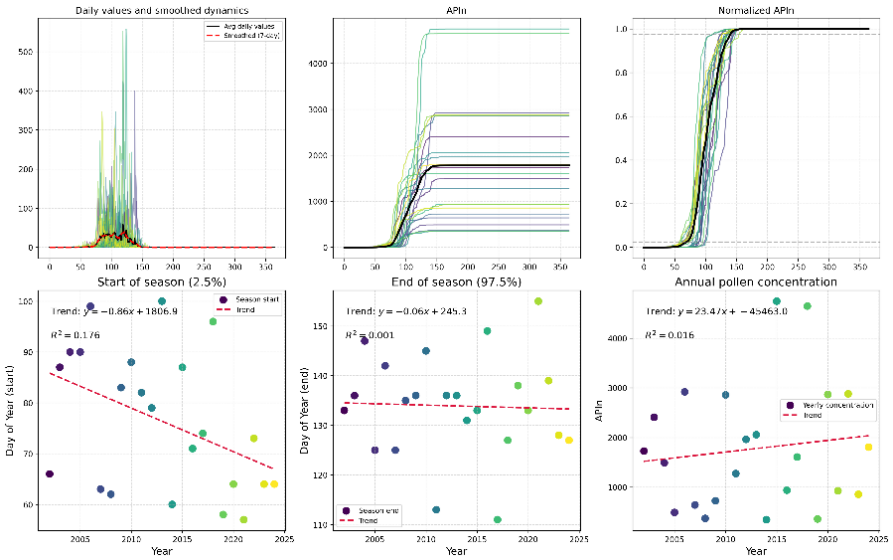

Figure S4j: Example of the pollen season analysis pipeline applied to *Fraxinus* spp. (ash) in Ljubljana. The top row presents the seasonal dynamics and data normalization: (upper left) daily pollen concentrations showing average values (black line) and 7-day smoothing (red dashed line); (upper middle) cumulative annual pollen totals; and (upper right) normalized cumulative sums used for phenological thresholding. The bottom row illustrates inter-annual trends over the 23-year period (2002-2024) for (lower left) season start day (2.5% threshold), (lower middle) season end day (97.5% threshold), and (lower right) the annual pollen integral (APIn). Linear regression lines and coefficients of determination (R^2) highlight a shift toward an earlier and more intense pollen season.

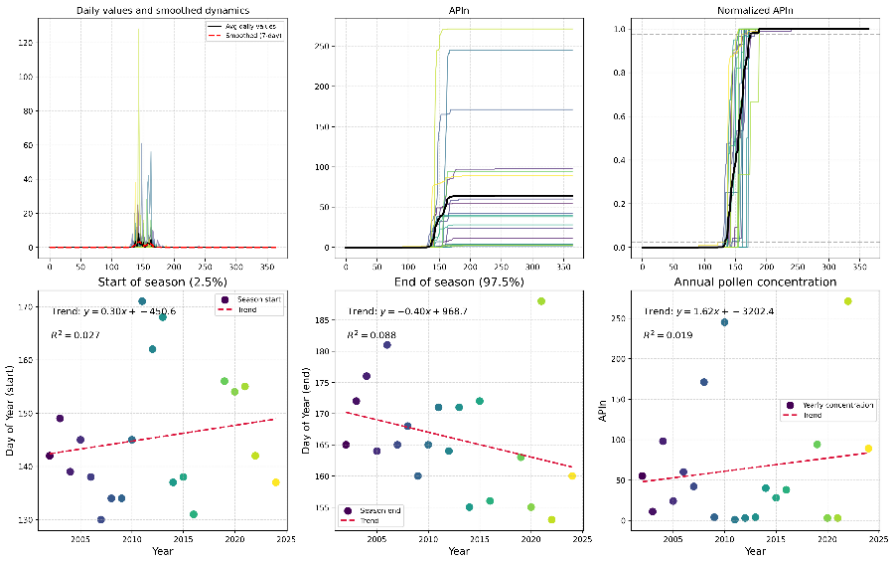

Figure S4k: Example of the pollen season analysis pipeline applied to *Olea* sp. (olive) in Ljubljana. The top row presents the seasonal dynamics and data normalization: (upper left) daily pollen concentrations showing average values (black line) and 7-day smoothing (red dashed line); (upper middle) cumulative annual pollen totals; and (upper right) normalized cumulative sums used for phenological thresholding. The bottom row illustrates inter-annual trends over the 23-year period (2002-2024) for (lower left) season start day (2.5% threshold), (lower middle) season end day (97.5% threshold), and (lower right) the annual pollen integral (APIn). Linear regression lines and coefficients of determination (R^2) highlight a shift toward an earlier and more intense pollen season.

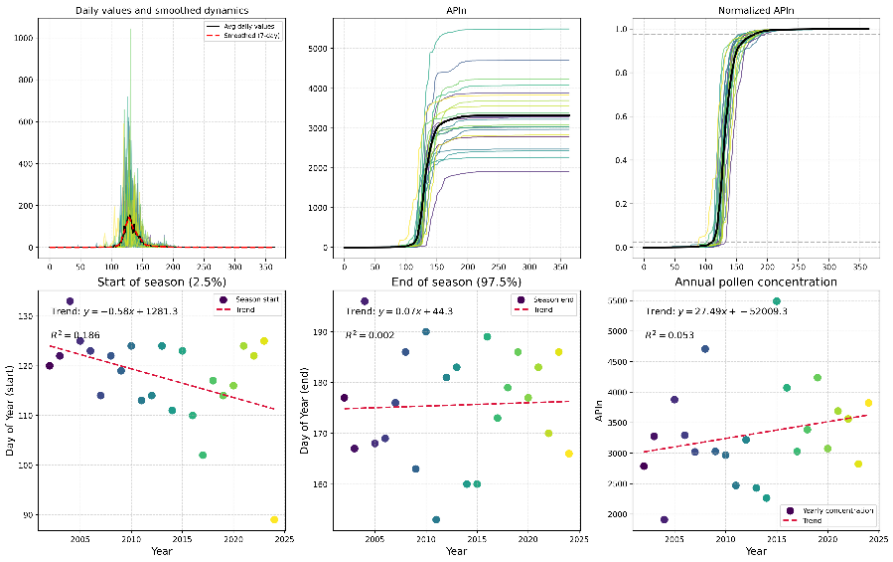

Figure S4l: Example of the pollen season analysis pipeline applied to *Pinus* spp. (pine) in Ljubljana. The top row presents the seasonal dynamics and data normalization: (upper left) daily pollen concentrations showing average values (black line) and 7-day smoothing (red dashed line); (upper middle) cumulative annual pollen totals; and (upper right) normalized cumulative sums used for phenological thresholding. The bottom row illustrates inter-annual trends over the 23-year period (2002-2024) for (lower left) season start day (2.5% threshold), (lower middle) season end day (97.5% threshold), and (lower right) the annual pollen integral (APIn). Linear regression lines and coefficients of determination (R^2) highlight a shift toward an earlier and more intense pollen season.

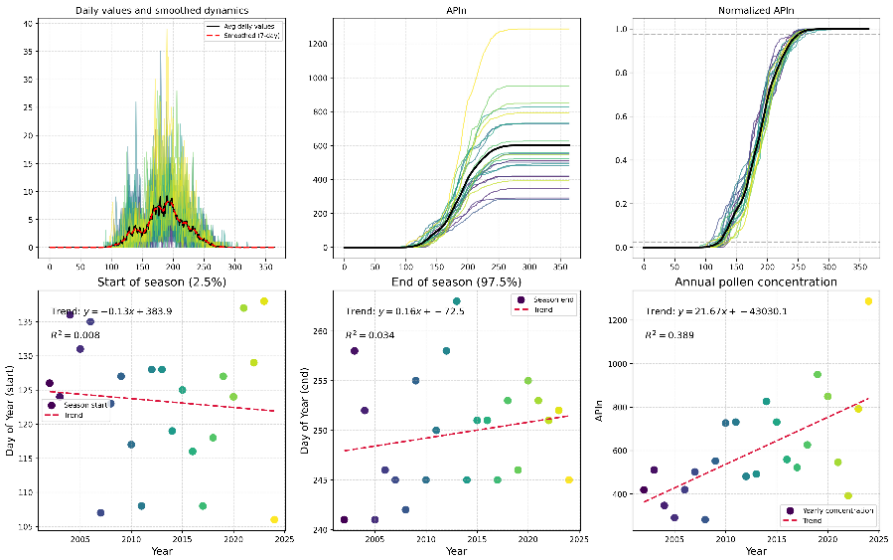

Figure S4m: Example of the pollen season analysis pipeline applied to *Plantago* spp. (plantain) in Ljubljana. The top row presents the seasonal dynamics and data normalization: (upper left) daily pollen concentrations showing average values (black line) and 7-day smoothing (red dashed line); (upper middle) cumulative annual pollen totals; and (upper right) normalized cumulative sums used for phenological thresholding. The bottom row illustrates inter-annual trends over the 23-year period (2002-2024) for (lower left) season start day (2.5% threshold), (lower middle) season end day (97.5% threshold), and (lower right) the annual pollen integral (APIn). Linear regression lines and coefficients of determination (R^2) highlight a shift toward an earlier and more intense pollen season.

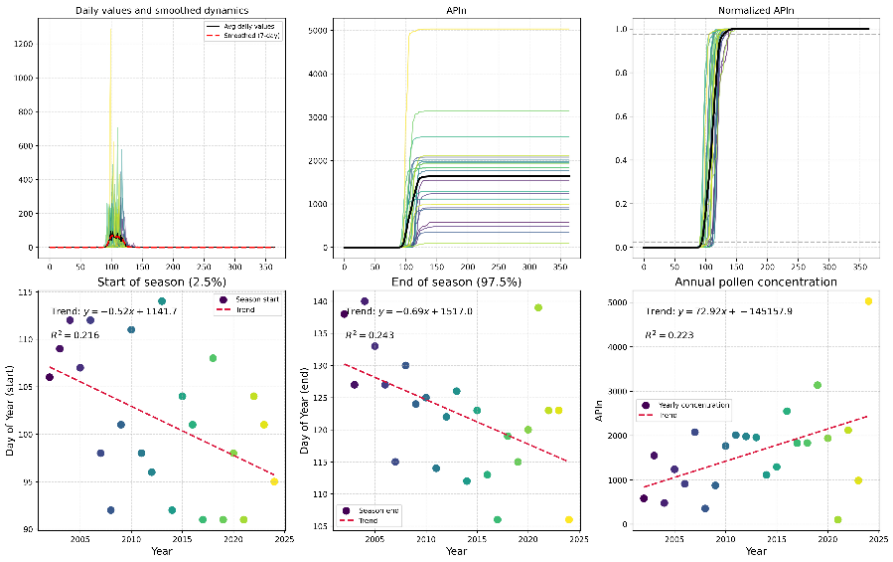

Figure S4n: Example of the pollen season analysis pipeline applied to *Platanus* spp. (plane tree) in Ljubljana. The top row presents the seasonal dynamics and data normalization: (upper left) daily pollen concentrations showing average values (black line) and 7-day smoothing (red dashed line); (upper middle) cumulative annual pollen totals; and (upper right) normalized cumulative sums used for phenological thresholding. The bottom row illustrates inter-annual trends over the 23-year period (2002-2024) for (lower left) season start day (2.5% threshold), (lower middle) season end day (97.5% threshold), and (lower right) the annual pollen integral (APIn). Linear regression lines and coefficients of determination (R^2) highlight a shift toward an earlier and more intense pollen season.

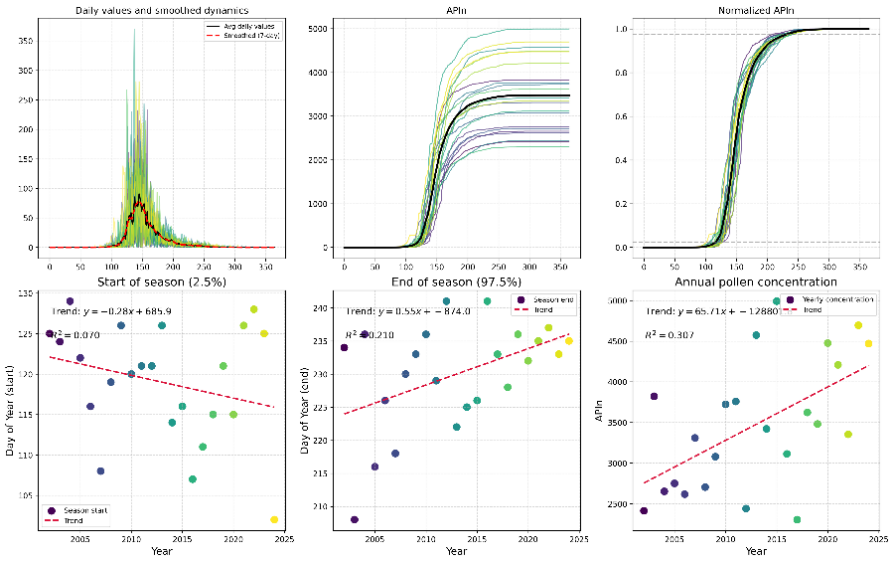

Figure S4o: Example of the pollen season analysis pipeline applied to Poaceae (grasses) in Ljubljana. The top row presents the seasonal dynamics and data normalization: (upper left) daily pollen concentrations showing average values (black line) and 7-day smoothing (red dashed line); (upper middle) cumulative annual pollen totals; and (upper right) normalized cumulative sums used for phenological thresholding. The bottom row illustrates inter-annual trends over the 23-year period (2002-2024) for (lower left) season start day (2.5% threshold), (lower middle) season end day (97.5% threshold), and (lower right) the annual pollen integral (APIn). Linear regression lines and coefficients of determination (R^2) highlight a shift toward an earlier and more intense pollen season.

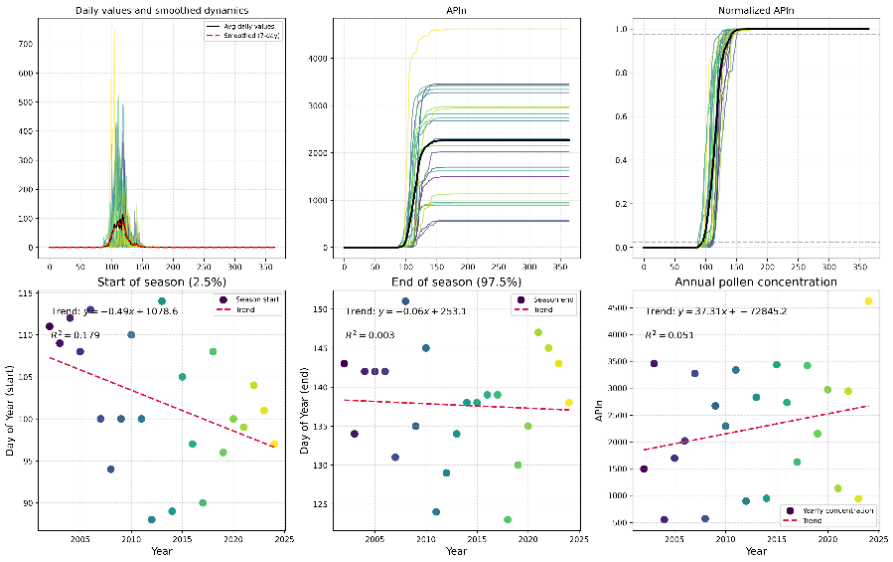

Figure S4p: Example of the pollen season analysis pipeline applied to *Quercus* spp. (oak) in Ljubljana. The top row presents the seasonal dynamics and data normalization: (upper left) daily pollen concentrations showing average values (black line) and 7-day smoothing (red dashed line); (upper middle) cumulative annual pollen totals; and (upper right) normalized cumulative sums used for phenological thresholding. The bottom row illustrates inter-annual trends over the 23-year period (2002-2024) for (lower left) season start day (2.5% threshold), (lower middle) season end day (97.5% threshold), and (lower right) the annual pollen integral (APIn). Linear regression lines and coefficients of determination (R^2) highlight a shift toward an earlier and more intense pollen season.

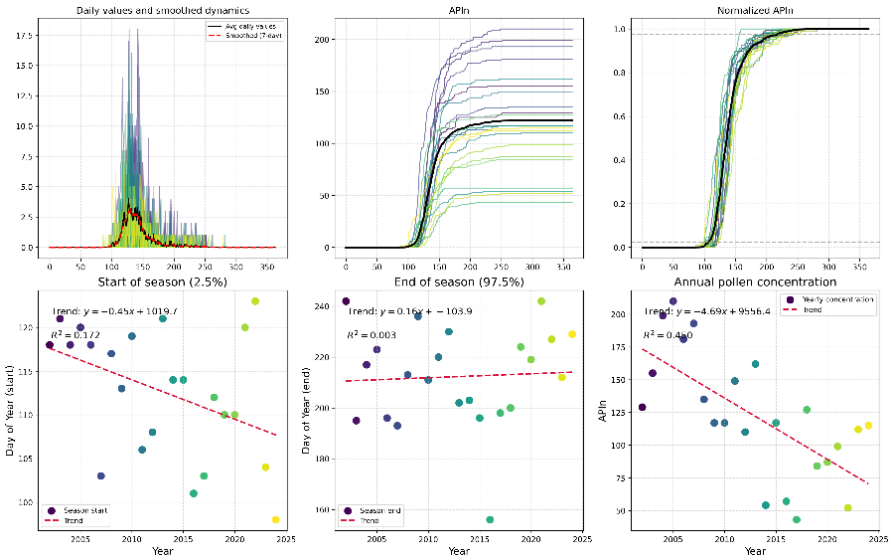

Figure S4q: Example of the pollen season analysis pipeline applied to *Rumex* spp. (dock) in Ljubljana. The top row presents the seasonal dynamics and data normalization: (upper left) daily pollen concentrations showing average values (black line) and 7-day smoothing (red dashed line); (upper middle) cumulative annual pollen totals; and (upper right) normalized cumulative sums used for phenological thresholding. The bottom row illustrates inter-annual trends over the 23-year period (2002-2024) for (lower left) season start day (2.5% threshold), (lower middle) season end day (97.5% threshold), and (lower right) the annual pollen integral (APIn). Linear regression lines and coefficients of determination (R^2) highlight a shift toward an earlier and more intense pollen season.

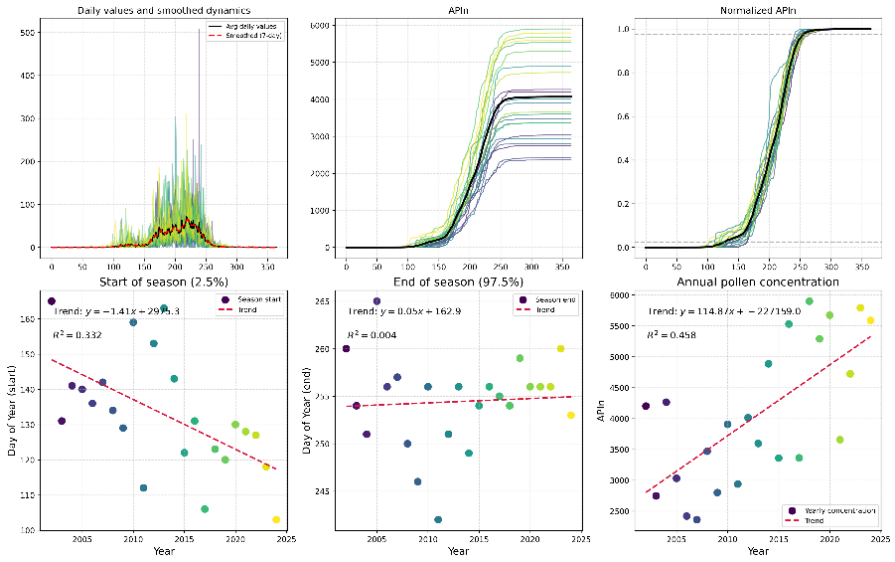

Figure S4r: Example of the pollen season analysis pipeline applied to Urticaceae (nettle) in Ljubljana. The top row presents the seasonal dynamics and data normalization: (upper left) daily pollen concentrations showing average values (black line) and 7-day smoothing (red dashed line); (upper middle) cumulative annual pollen totals; and (upper right) normalized cumulative sums used for phenological thresholding. The bottom row illustrates inter-annual trends over the 23-year period (2002-2024) for (lower left) season start day (2.5% threshold), (lower middle) season end day (97.5% threshold), and (lower right) the annual pollen integral (APIn). Linear regression lines and coefficients of determination (R^2) highlight a shift toward an earlier and more intense pollen season.

Maribor Analysis Results

This section contains all analysis results for Maribor, including global overviews, data completeness assessments, statistical analyses, and type-specific results.

Global Overview Analysis

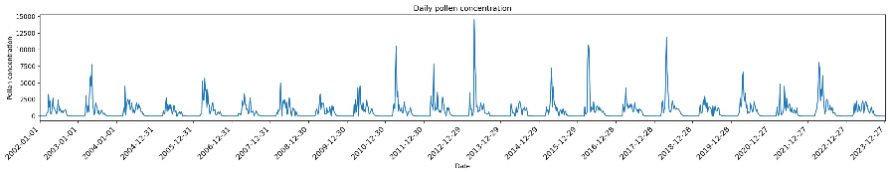

Figure S5a: Global Overview of Pollen Record in Maribor, showing the distribution and abundance of pollen species across different time periods.

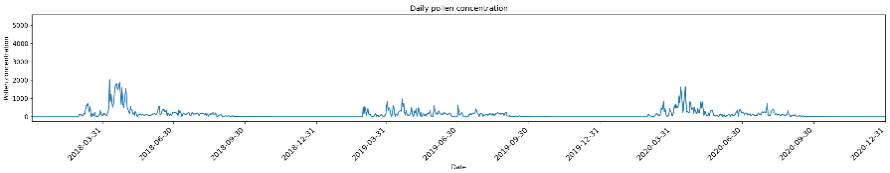

Figure S5b: Global overview pollen diagram for Maribor, Slovenia, illustrating the seasonal patterns of major tree and grass pollen species in the region.

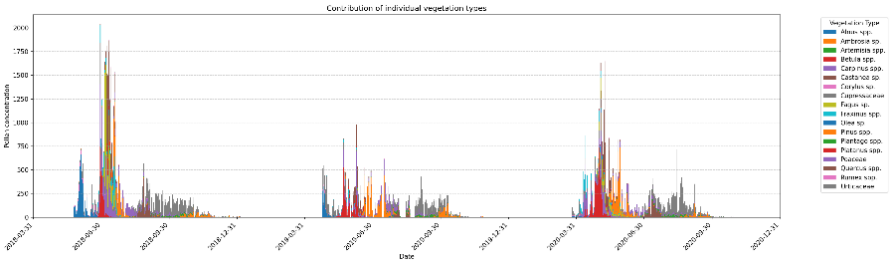

Figure S5c: Global overview of pollen records from Maribor, Slovenia, highlighting seasonal patterns and species distribution across the region.

Data Completeness Assessment

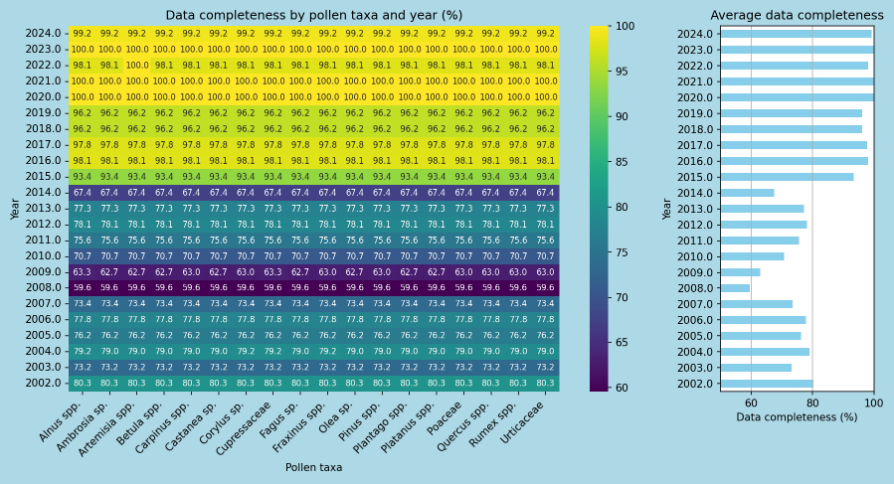

Figure S6a: Annual pollen data completeness assessment for Maribor, Slovenia, showing the percentage of pollen samples collected and analyzed each month over a one-year period.

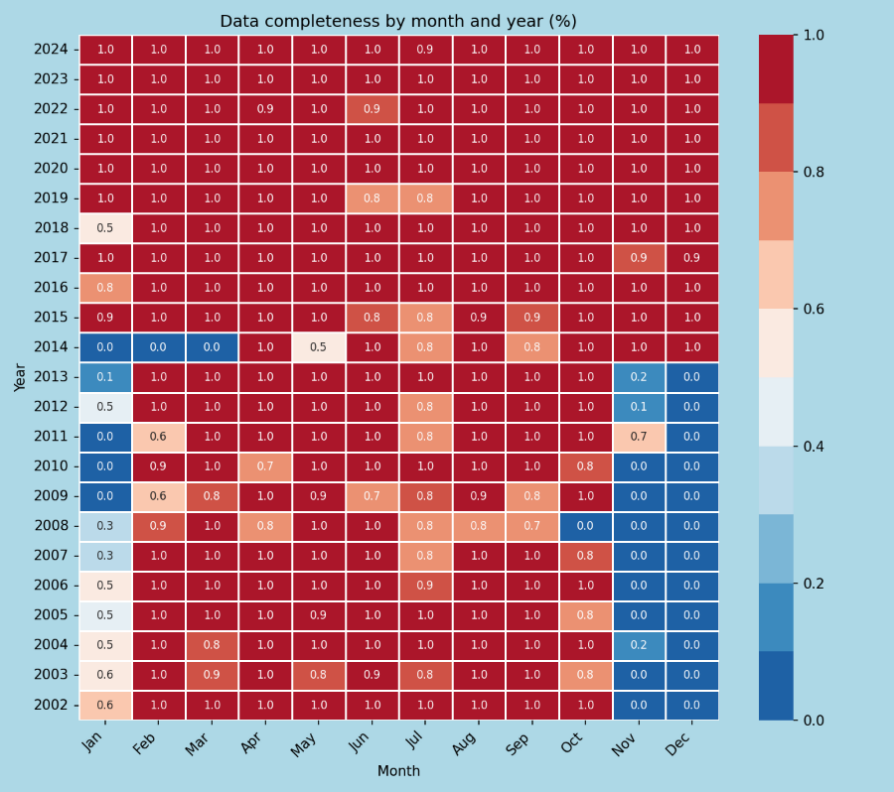

Figure S6b: Monthly pollen data completeness assessment for Ljubljana, Slovenia. The figure displays the proportion of dataset completeness for individual months of a given year. The color-bar on the right displays the color mapping of completeness values, where red indicates complete data (1.0 or 100%), and lighter shades represent incomplete data, with blue indicating the lowest completeness values (0.4 or 40%). Each cell shows the completeness proportion for a specific month-year combination, revealing that most months have complete data (1.0).

Pripombe dodal [UR4]: Maribor?

Season statistics for Maribor, Slovenia

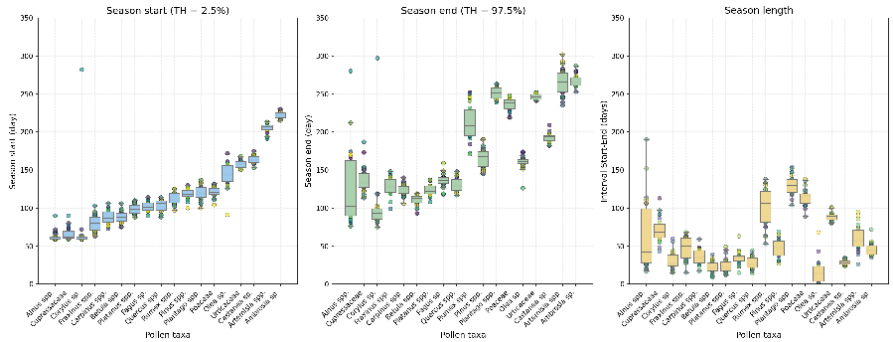

Figure S7: Pollen season metrics across taxa in Maribor, Slovenia. Box plots showing (left) season start day expressed as day of year using the 2.5% threshold of cumulative annual pollen count, (middle) season end day using the 97.5% threshold, and (right) season length in days calculated as the difference between season end and start dates. Each box represents the interquartile range (IQR) with the median shown as a horizontal line, whiskers extend to 1.5×IQR, and outliers are shown as individual points. Pollen taxa are ordered chronologically based on their typical season timing, with early-season taxa (*Corylus*, *Alnus*) on the left and late-season taxa (*Artemisia*, *Ambrosia*) on the right.

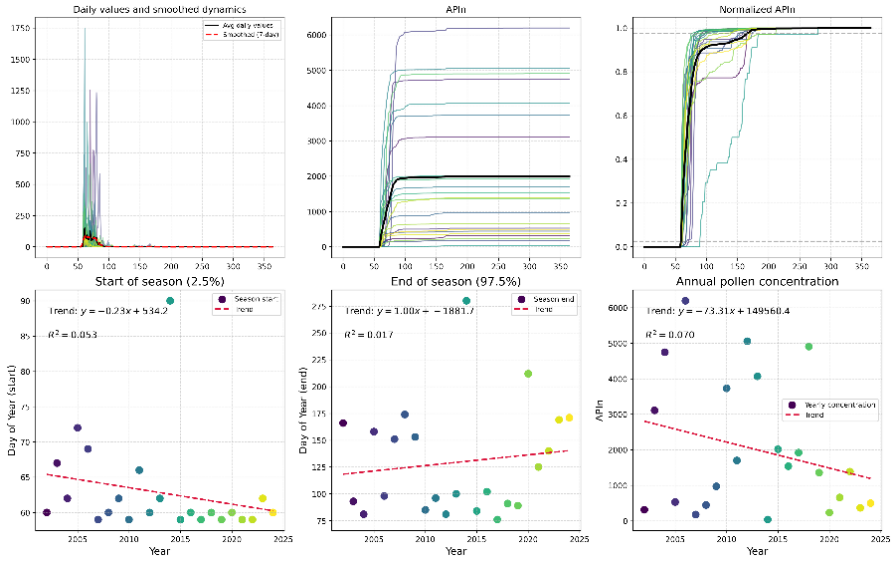

Figure S8a: Example of the pollen season analysis pipeline applied to *Alnus* spp. (alder) in Maribor. The top row presents the seasonal dynamics and data normalization: (upper left) daily pollen concentrations showing average values (black line) and 7-day smoothing (red dashed line); (upper middle) cumulative annual pollen totals; and (upper right) normalized cumulative sums used for phenological thresholding. The bottom row illustrates inter-annual trends over the 23-year period (2002-2024) for (lower left) season start day (2.5% threshold), (lower middle) season end day (97.5% threshold), and (lower right) the annual pollen integral (APIn). Linear regression lines and coefficients of determination (R^2) highlight a shift toward an earlier and more intense pollen season.

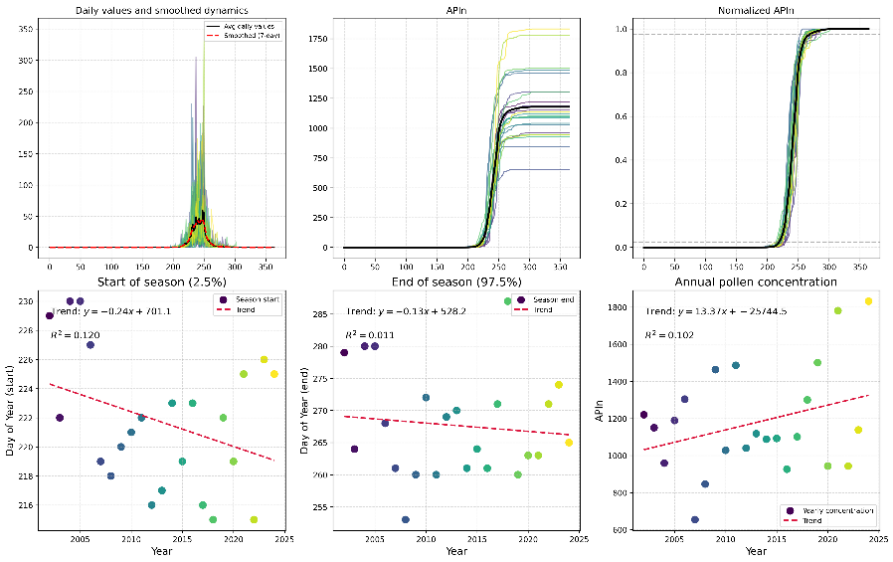

Figure S8b: Example of the pollen season analysis pipeline applied to *Ambrosia* sp. (ragweed) in Maribor. The top row presents the seasonal dynamics and data normalization: (upper left) daily pollen concentrations showing average values (black line) and 7-day smoothing (red dashed line); (upper middle) cumulative annual pollen totals; and (upper right) normalized cumulative sums used for phenological thresholding. The bottom row illustrates inter-annual trends over the 23-year period (2002-2024) for (lower left) season start day (2.5% threshold), (lower middle) season end day (97.5% threshold), and (lower right) the annual pollen integral (APIn). Linear regression lines and coefficients of determination (R^2) highlight a shift toward an earlier and more intense pollen season.

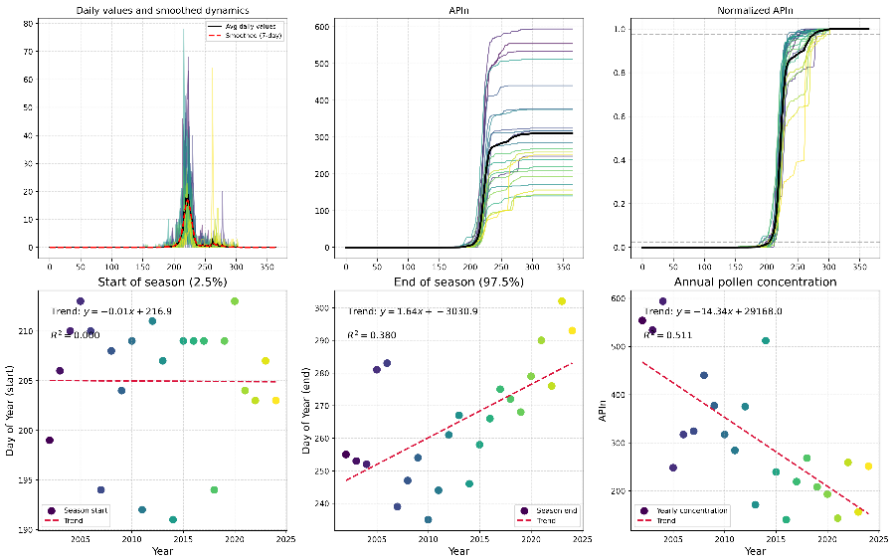

Figure S8c: Example of the pollen season analysis pipeline applied to *Artemisia* spp. (mugwort) in Maribor. The top row presents the seasonal dynamics and data normalization: (upper left) daily pollen concentrations showing average values (black line) and 7-day smoothing (red dashed line); (upper middle) cumulative annual pollen totals; and (upper right) normalized cumulative sums used for phenological thresholding. The bottom row illustrates inter-annual trends over the 23-year period (2002-2024) for (lower left) season start day (2.5% threshold), (lower middle) season end day (97.5% threshold), and (lower right) the annual pollen integral (APIn). Linear regression lines and coefficients of determination (R^2) highlight a shift toward an earlier and more intense pollen season.

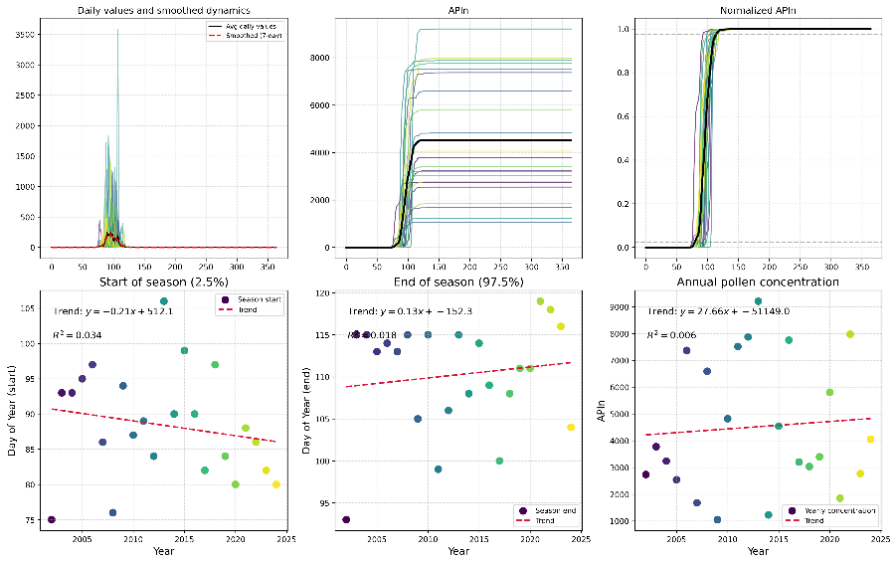

Figure S8d: Example of the pollen season analysis pipeline applied to *Betula* spp. (birch) in Maribor. The top row presents the seasonal dynamics and data normalization: (upper left) daily pollen concentrations showing average values (black line) and 7-day smoothing (red dashed line); (upper middle) cumulative annual pollen totals; and (upper right) normalized cumulative sums used for phenological thresholding. The bottom row illustrates inter-annual trends over the 23-year period (2002-2024) for (lower left) season start day (2.5% threshold), (lower middle) season end day (97.5% threshold), and (lower right) the annual pollen integral (APIn). Linear regression lines and coefficients of determination (R^2) highlight a shift toward an earlier and more intense pollen season.

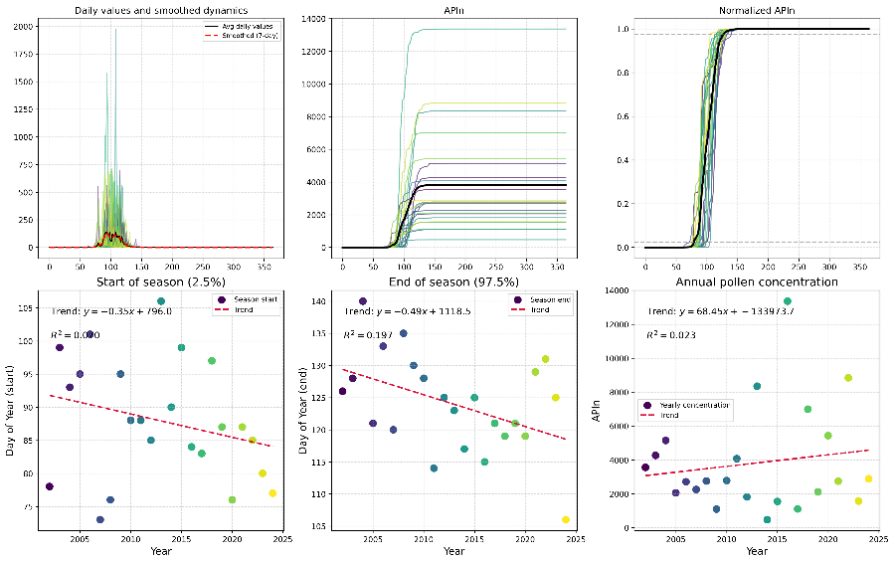

Figure S8e: Example of the pollen season analysis pipeline applied to *Carpinus* spp./*Ostrya* spp. (hornbeam/hop-hornbeam) in Maribor. The top row presents the seasonal dynamics and data normalization: (upper left) daily pollen concentrations showing average values (black line) and 7-day smoothing (red dashed line); (upper middle) cumulative annual pollen totals; and (upper right) normalized cumulative sums used for phenological thresholding. The bottom row illustrates inter-annual trends over the 23-year period (2002-2024) for (lower left) season start day (2.5% threshold), (lower middle) season end day (97.5% threshold), and (lower right) the annual pollen integral (APIn). Linear regression lines and coefficients of determination (R^2) highlight a shift toward an earlier and more intense pollen season.

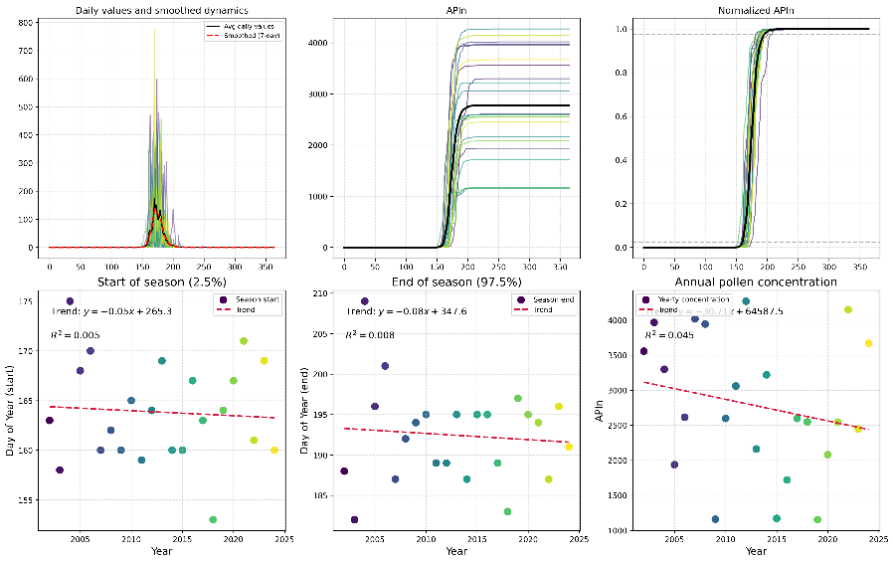

Figure S8f: Example of the pollen season analysis pipeline applied to *Castanea* sp. (sweet chestnut) in Maribor. The top row presents the seasonal dynamics and data normalization: (upper left) daily pollen concentrations showing average values (black line) and 7-day smoothing (red dashed line); (upper middle) cumulative annual pollen totals; and (upper right) normalized cumulative sums used for phenological thresholding. The bottom row illustrates inter-annual trends over the 23-year period (2002-2024) for (lower left) season start day (2.5% threshold), (lower middle) season end day (97.5% threshold), and (lower right) the annual pollen integral (APIn). Linear regression lines and coefficients of determination (R^2) highlight a shift toward an earlier and more intense pollen season.

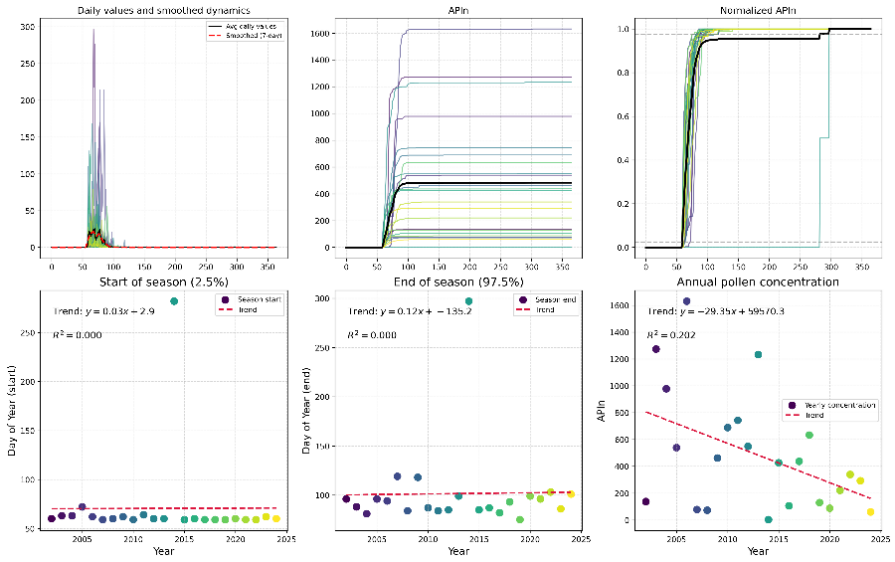

Figure S8g: Example of the pollen season analysis pipeline applied to *Corylus* sp. (hazel) in Maribor. The top row presents the seasonal dynamics and data normalization: (upper left) daily pollen concentrations showing average values (black line) and 7-day smoothing (red dashed line); (upper middle) cumulative annual pollen totals; and (upper right) normalized cumulative sums used for phenological thresholding. The bottom row illustrates inter-annual trends over the 23-year period (2002-2024) for (lower left) season start day (2.5% threshold), (lower middle) season end day (97.5% threshold), and (lower right) the annual pollen integral (APIn). Linear regression lines and coefficients of determination (R^2) highlight a shift toward an earlier and more intense pollen season.

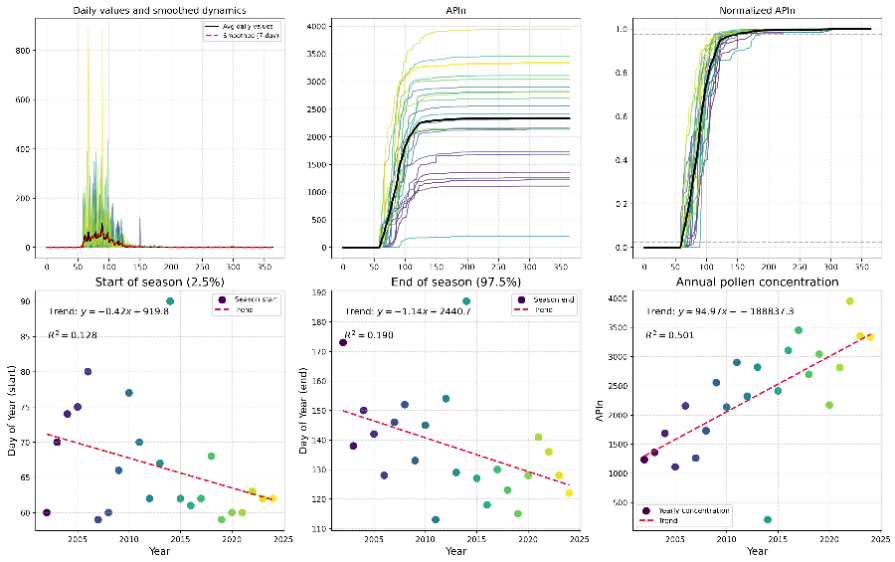

Figure S8h: Example of the pollen season analysis pipeline applied to Cupressaceae/Taxaceae (cypress/yew) in Maribor. The top row presents the seasonal dynamics and data normalization: (upper left) daily pollen concentrations showing average values (black line) and 7-day smoothing (red dashed line); (upper middle) cumulative annual pollen totals; and (upper right) normalized cumulative sums used for phenological thresholding. The bottom row illustrates inter-annual trends over the 23-year period (2002-2024) for (lower left) season start day (2.5% threshold), (lower middle) season end day (97.5% threshold), and (lower right) the annual pollen integral (APIn). Linear regression lines and coefficients of determination (R^2) highlight a shift toward an earlier and more intense pollen season.

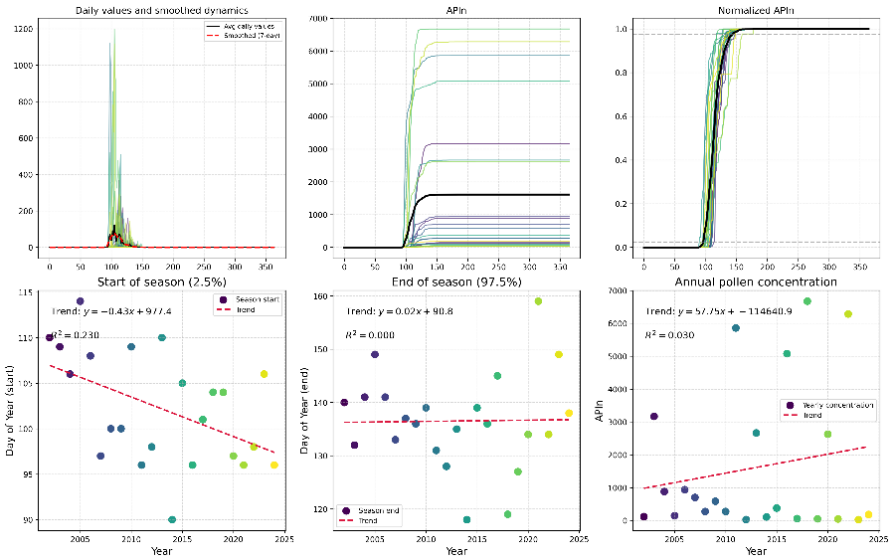

Figure S8i: Example of the pollen season analysis pipeline applied to *Fagus* sp. (beech) in Maribor. The top row presents the seasonal dynamics and data normalization: (upper left) daily pollen concentrations showing average values (black line) and 7-day smoothing (red dashed line); (upper middle) cumulative annual pollen totals; and (upper right) normalized cumulative sums used for phenological thresholding. The bottom row illustrates inter-annual trends over the 23-year period (2002-2024) for (lower left) season start day (2.5% threshold), (lower middle) season end day (97.5% threshold), and (lower right) the annual pollen integral (APIn). Linear regression lines and coefficients of determination (R^2) highlight a shift toward an earlier and more intense pollen season.

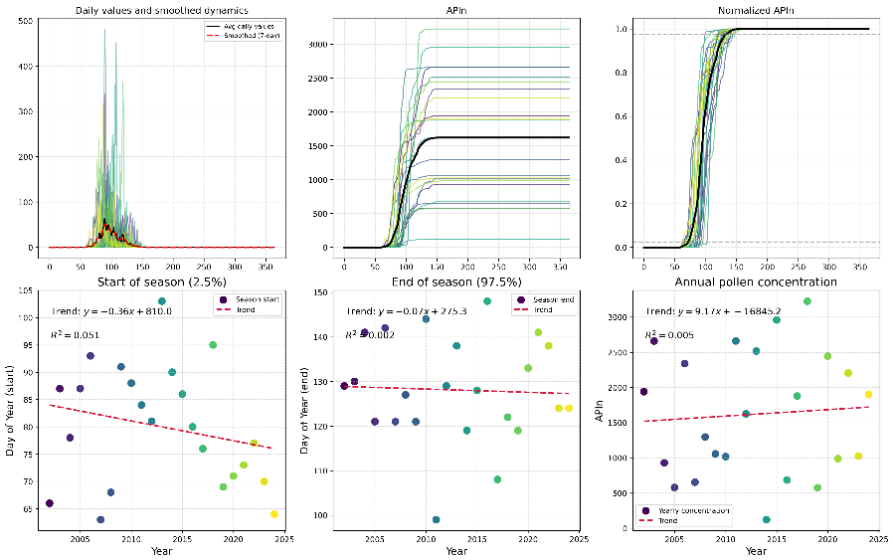

Figure S8j: Example of the pollen season analysis pipeline applied to *Fraxinus* spp. (ash) in Maribor. The top row presents the seasonal dynamics and data normalization: (upper left) daily pollen concentrations showing average values (black line) and 7-day smoothing (red dashed line); (upper middle) cumulative annual pollen totals; and (upper right) normalized cumulative sums used for phenological thresholding. The bottom row illustrates inter-annual trends over the 23-year period (2002-2024) for (lower left) season start day (2.5% threshold), (lower middle) season end day (97.5% threshold), and (lower right) the annual pollen integral (APIn). Linear regression lines and coefficients of determination (R^2) highlight a shift toward an earlier and more intense pollen season.

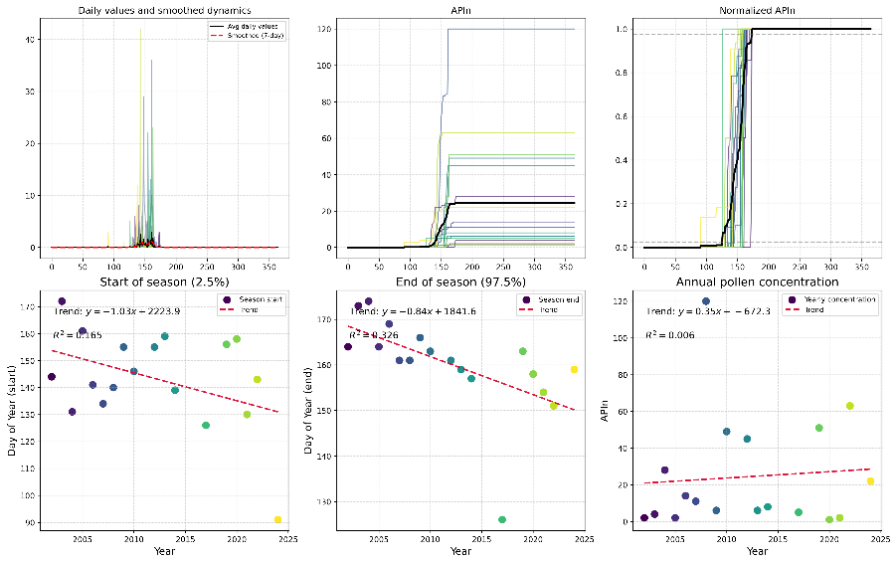

Figure S8k: Example of the pollen season analysis pipeline applied to *Olea* sp. (olive) in Maribor. The top row presents the seasonal dynamics and data normalization: (upper left) daily pollen concentrations showing average values (black line) and 7-day smoothing (red dashed line); (upper middle) cumulative annual pollen totals; and (upper right) normalized cumulative sums used for phenological thresholding. The bottom row illustrates inter-annual trends over the 23-year period (2002-2024) for (lower left) season start day (2.5% threshold), (lower middle) season end day (97.5% threshold), and (lower right) the annual pollen integral (APIn). Linear regression lines and coefficients of determination (R^2) highlight a shift toward an earlier and more intense pollen season.

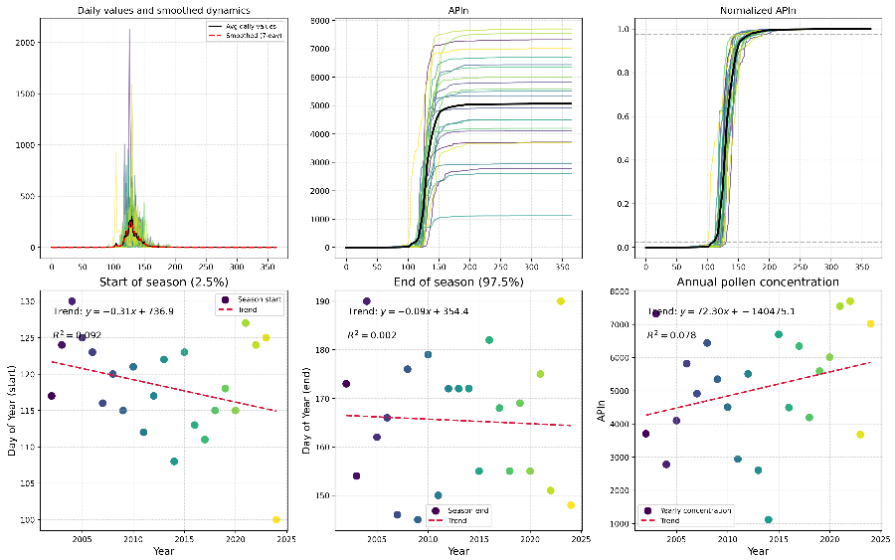

Figure S8l: Example of the pollen season analysis pipeline applied to *Pinus* spp. (pine) in Maribor. The top row presents the seasonal dynamics and data normalization: (upper left) daily pollen concentrations showing average values (black line) and 7-day smoothing (red dashed line); (upper middle) cumulative annual pollen totals; and (upper right) normalized cumulative sums used for phenological thresholding. The bottom row illustrates inter-annual trends over the 23-year period (2002-2024) for (lower left) season start day (2.5% threshold), (lower middle) season end day (97.5% threshold), and (lower right) the annual pollen integral (APIn). Linear regression lines and coefficients of determination (R^2) highlight a shift toward an earlier and more intense pollen season.

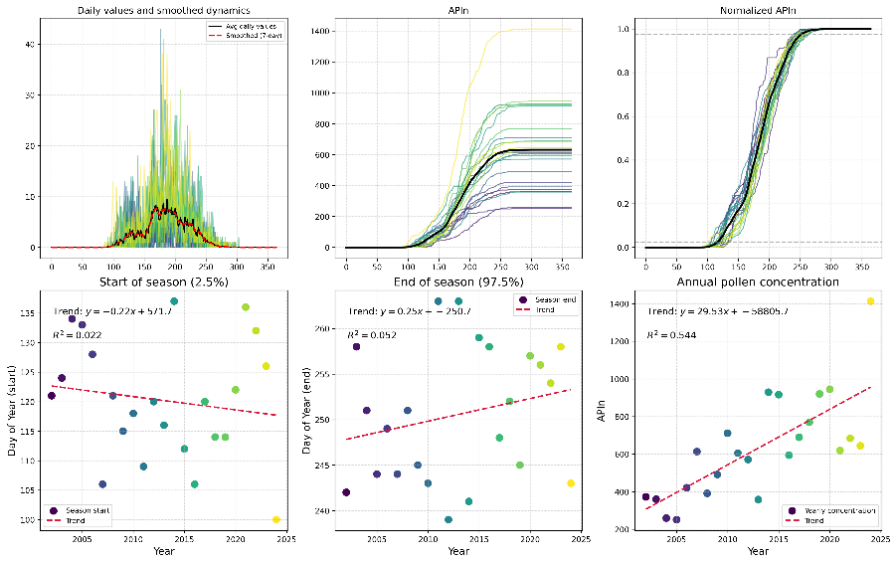

Figure S8m: Example of the pollen season analysis pipeline applied to *Plantago* spp. (plantain) in Maribor. The top row presents the seasonal dynamics and data normalization: (upper left) daily pollen concentrations showing average values (black line) and 7-day smoothing (red dashed line); (upper middle) cumulative annual pollen totals; and (upper right) normalized cumulative sums used for phenological thresholding. The bottom row illustrates inter-annual trends over the 23-year period (2002-2024) for (lower left) season start day (2.5% threshold), (lower middle) season end day (97.5% threshold), and (lower right) the annual pollen integral (APIn). Linear regression lines and coefficients of determination (R^2) highlight a shift toward an earlier and more intense pollen season.

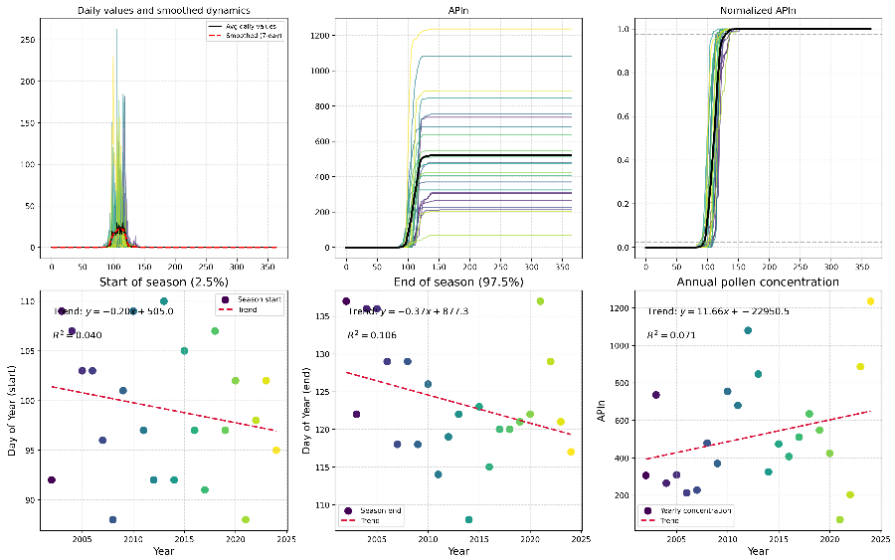

Figure S8n: Example of the pollen season analysis pipeline applied to *Platanus* spp. (plane tree) in Maribor. The top row presents the seasonal dynamics and data normalization: (upper left) daily pollen concentrations showing average values (black line) and 7-day smoothing (red dashed line); (upper middle) cumulative annual pollen totals; and (upper right) normalized cumulative sums used for phenological thresholding. The bottom row illustrates inter-annual trends over the 23-year period (2002-2024) for (lower left) season start day (2.5% threshold), (lower middle) season end day (97.5% threshold), and (lower right) the annual pollen integral (APIn). Linear regression lines and coefficients of determination (R^2) highlight a shift toward an earlier and more intense pollen season.

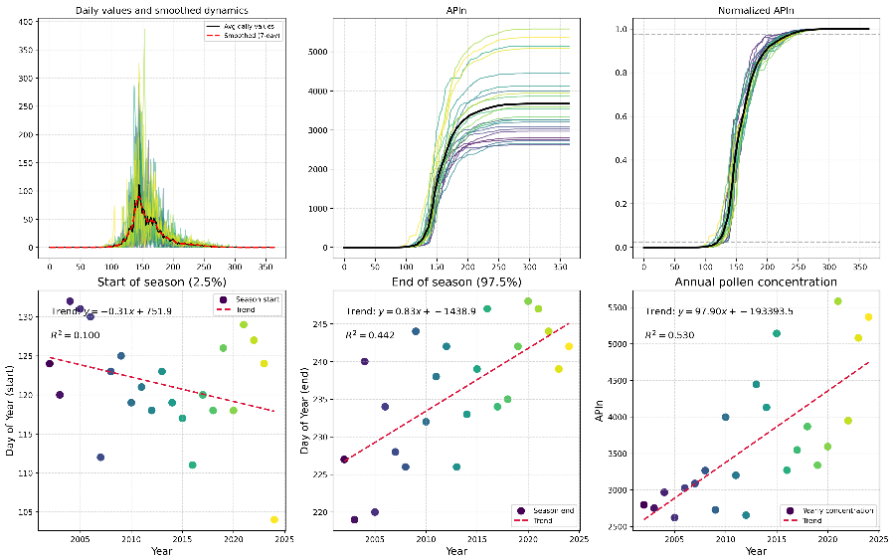

Figure S8o: Example of the pollen season analysis pipeline applied to Poaceae (grasses) in Maribor. The top row presents the seasonal dynamics and data normalization: (upper left) daily pollen concentrations showing average values (black line) and 7-day smoothing (red dashed line); (upper middle) cumulative annual pollen totals; and (upper right) normalized cumulative sums used for phenological thresholding. The bottom row illustrates inter-annual trends over the 23-year period (2002-2024) for (lower left) season start day (2.5% threshold), (lower middle) season end day (97.5% threshold), and (lower right) the annual pollen integral (APIn). Linear regression lines and coefficients of determination (R^2) highlight a shift toward an earlier and more intense pollen season.

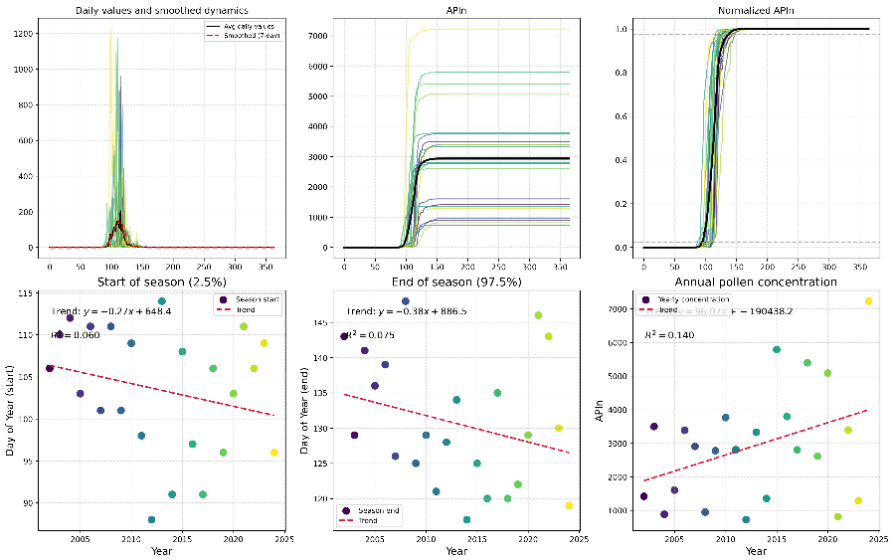

Figure S8p: Example of the pollen season analysis pipeline applied to *Quercus* spp. (oak) in Maribor. The top row presents the seasonal dynamics and data normalization: (upper left) daily pollen concentrations showing average values (black line) and 7-day smoothing (red dashed line); (upper middle) cumulative annual pollen totals; and (upper right) normalized cumulative sums used for phenological thresholding. The bottom row illustrates inter-annual trends over the 23-year period (2002-2024) for (lower left) season start day (2.5% threshold), (lower middle) season end day (97.5% threshold), and (lower right) the annual pollen integral (APIn). Linear regression lines and coefficients of determination (R^2) highlight a shift toward an earlier and more intense pollen season.

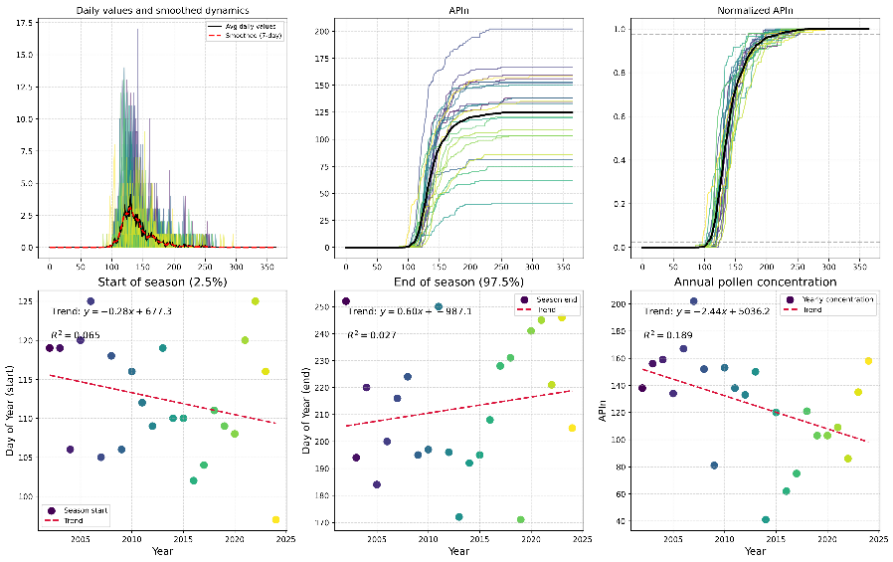

Figure S8q: Example of the pollen season analysis pipeline applied to *Rumex* spp. (dock) in Maribor. The top row presents the seasonal dynamics and data normalization: (upper left) daily pollen concentrations showing average values (black line) and 7-day smoothing (red dashed line); (upper middle) cumulative annual pollen totals; and (upper right) normalized cumulative sums used for phenological thresholding. The bottom row illustrates inter-annual trends over the 23-year period (2002-2024) for (lower left) season start day (2.5% threshold), (lower middle) season end day (97.5% threshold), and (lower right) the annual pollen integral (APIn). Linear regression lines and coefficients of determination (R^2) highlight a shift toward an earlier and more intense pollen season.

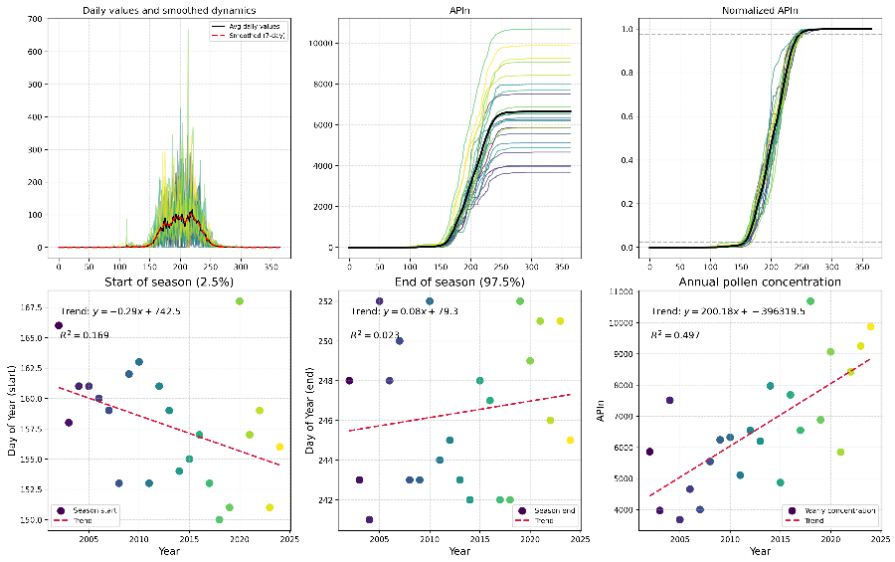

Figure S8r: Example of the pollen season analysis pipeline applied to Urticaceae (nettle) in Maribor. The top row presents the seasonal dynamics and data normalization: (upper left) daily pollen concentrations showing average values (black line) and 7-day smoothing (red dashed line); (upper middle) cumulative annual pollen totals; and (upper right) normalized cumulative sums used for phenological thresholding. The bottom row illustrates inter-annual trends over the 23-year period (2002-2024) for (lower left) season start day (2.5% threshold), (lower middle) season end day (97.5% threshold), and (lower right) the annual pollen integral (APIn). Linear regression lines and coefficients of determination (R^2) highlight a shift toward an earlier and more intense pollen season.

Primorje Analysis Results

This section contains all analysis results for Primorje, including global overviews, data completeness assessments, statistical analyses, and type-specific results.

Global Overview Analysis

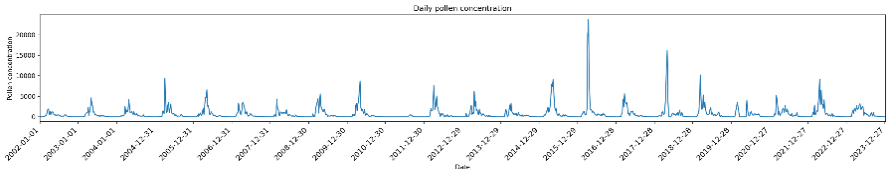

Figure S9a: Global Overview of Pollen Record in Primorje, showing the distribution and abundance of pollen species across different time periods.

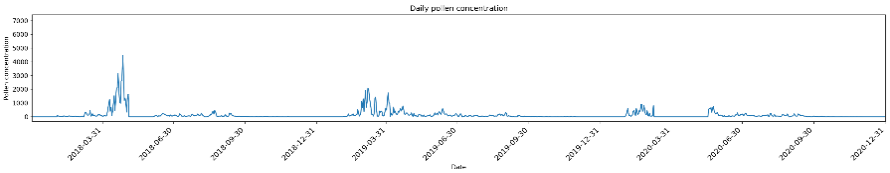

Figure S9b: Global overview pollen diagram for Primorje, Slovenia, illustrating the seasonal patterns of major tree and grass pollen species in the region.

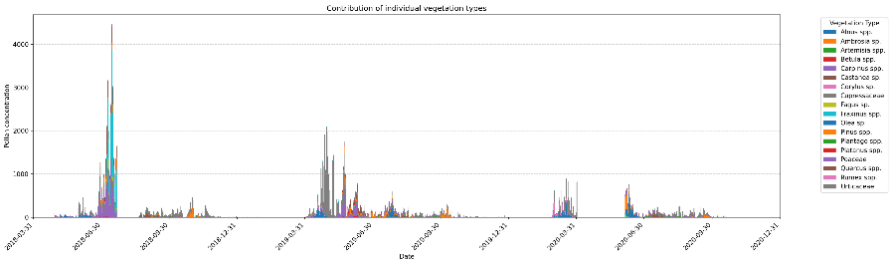

Figure S9c: Global overview of pollen records from Primorje, Slovenia, highlighting seasonal patterns and species distribution across the region.

Data Completeness Assessment

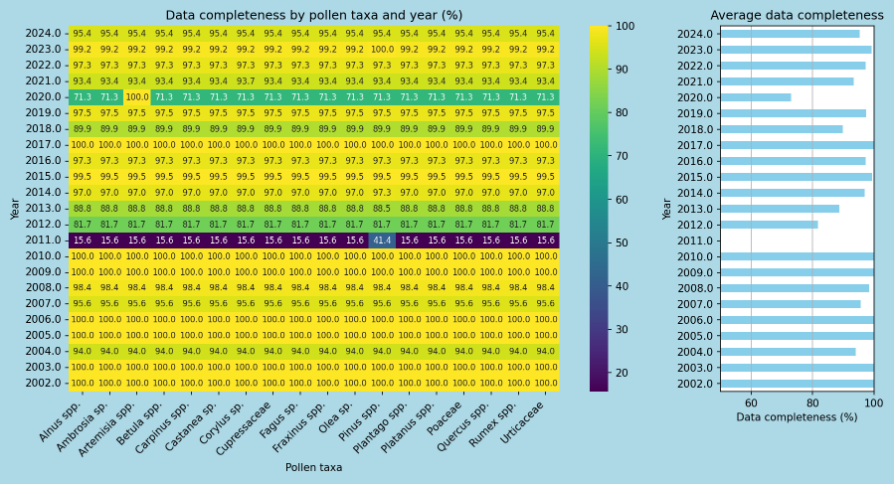

Figure S10a: Annual pollen data completeness assessment for Primorje, Slovenia, showing the percentage of pollen samples collected and analyzed each month over a one-year period.

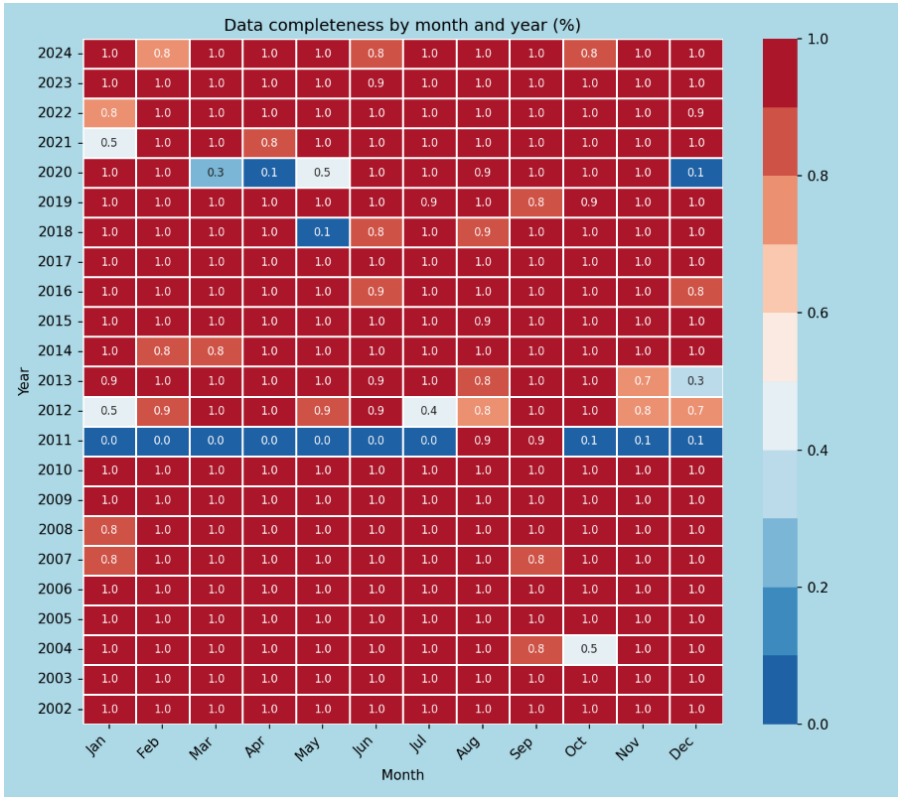

Figure S10b: Monthly pollen data completeness assessment for Primorje, Slovenia. The figure displays the proportion of dataset completeness for individual months of a given year. The color-bar on the right displays the color mapping of completeness values, where red indicates complete data (1.0 or 100%), and lighter shades represent incomplete data, with blue indicating the lowest completeness values (0.4 or 40%). Each cell shows the completeness proportion for a specific month-year combination, revealing that most months have complete data (1.0).

Season statistics for Primorje, Slovenia

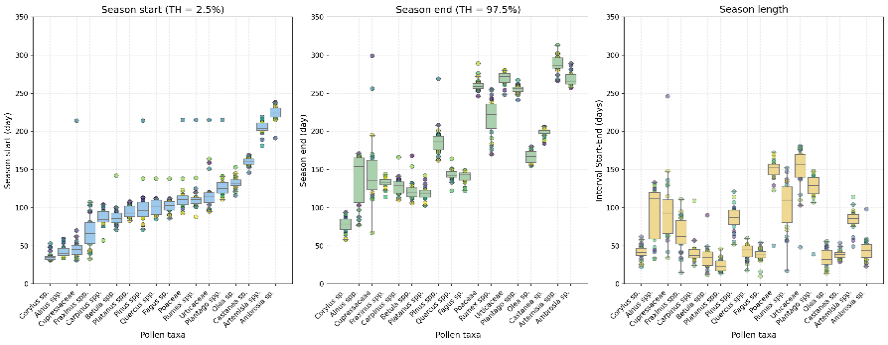

Figure S11: Pollen season metrics across taxa in Primorje, Slovenia. Box plots showing (left) season start day expressed as day of year using the 2.5% threshold of cumulative annual pollen count, (middle) season end day using the 97.5% threshold, and (right) season length in days calculated as the difference between season end and start dates. Each box represents the interquartile range (IQR) with the median shown as a horizontal line, whiskers extend to 1.5×IQR, and outliers are shown as individual points. Pollen taxa are ordered chronologically based on their typical season timing, with early-season taxa (*Corylus*, *Alnus*) on the left and late-season taxa (*Artemisia*, *Ambrosia*) on the right.

Pollen Taxa-Specific Analysis for Primorje

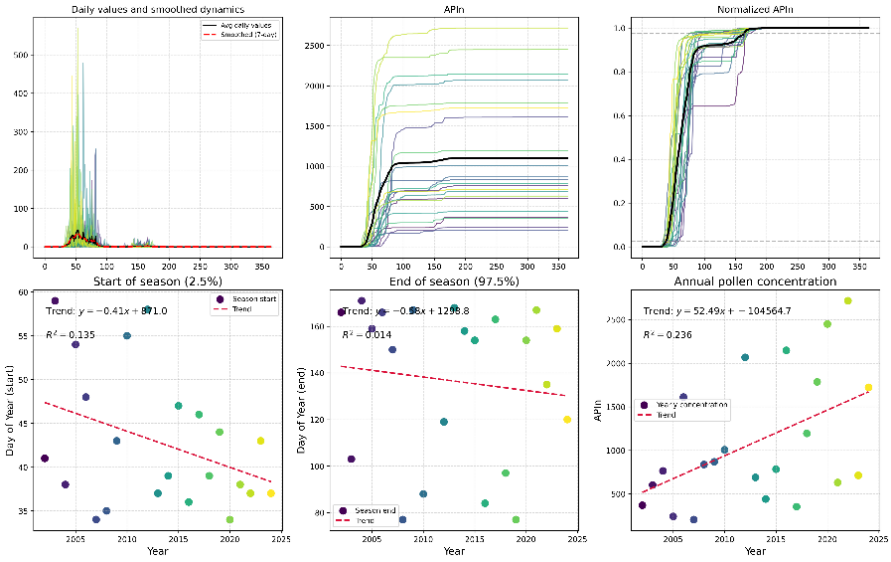

Figure S12a: Example of the pollen season analysis pipeline applied to *Alnus* spp. (alder) in Primorje. The top row presents the seasonal dynamics and data normalization: (upper left) daily pollen concentrations showing average values (black line) and 7-day smoothing (red dashed line); (upper middle) cumulative annual pollen totals; and (upper right) normalized cumulative sums used for phenological thresholding. The bottom row illustrates inter-annual trends over the 23-year period (2002-2024) for (lower left) season start day (2.5% threshold), (lower middle) season end day (97.5% threshold), and (lower right) the annual pollen integral (APIn). Linear regression lines and coefficients of determination (R^2) highlight a shift toward an earlier and more intense pollen season.

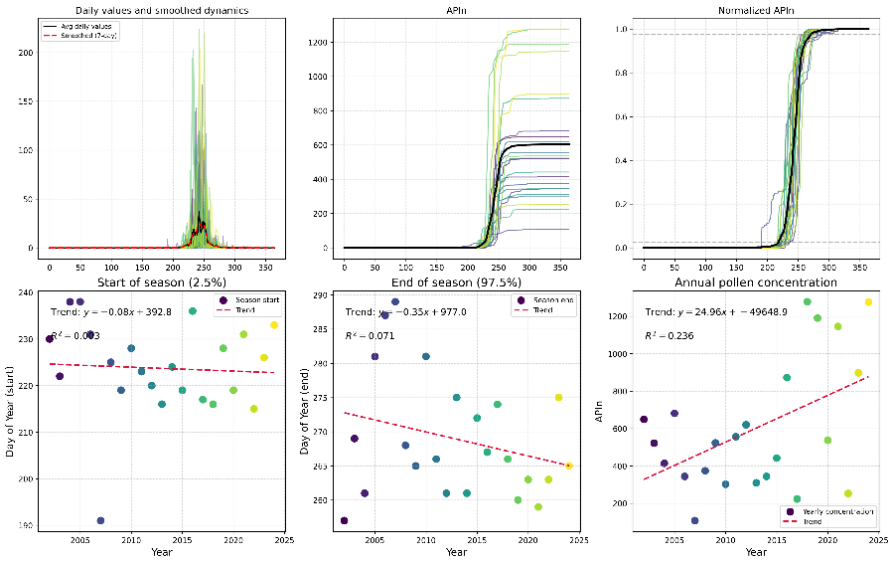

Figure S12b: Example of the pollen season analysis pipeline applied to *Ambrosia* sp. (ragweed) in Primorje. The top row presents the seasonal dynamics and data normalization: (upper left) daily pollen concentrations showing average values (black line) and 7-day smoothing (red dashed line); (upper middle) cumulative annual pollen totals; and (upper right) normalized cumulative sums used for phenological thresholding. The bottom row illustrates inter-annual trends over the 23-year period (2002-2024) for (lower left) season start day (2.5% threshold), (lower middle) season end day (97.5% threshold), and (lower right) the annual pollen integral (APIn). Linear regression lines and coefficients of determination (R^2) highlight a shift toward an earlier and more intense pollen season.

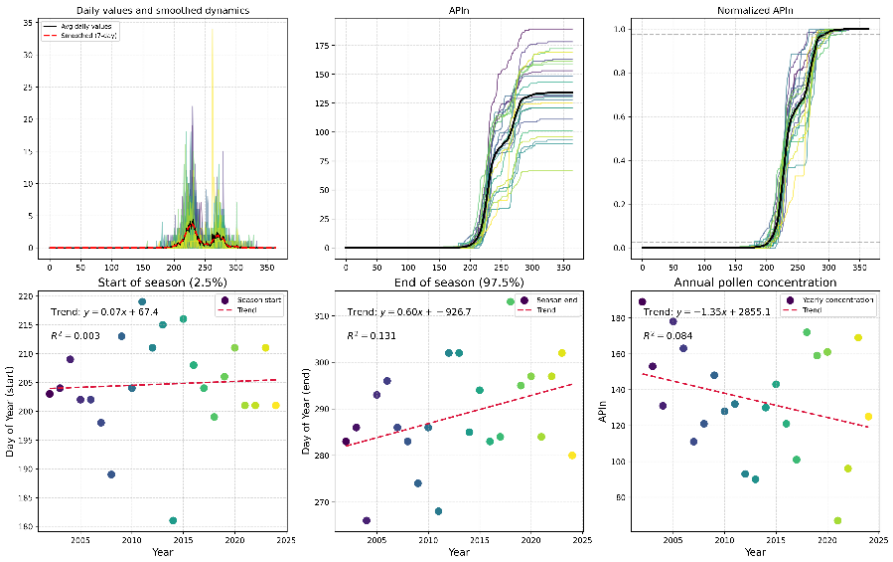

Figure S12c: Example of the pollen season analysis pipeline applied to Artemisia spp. (mugwort) in Primorje. The top row presents the seasonal dynamics and data normalization: (upper left) daily pollen concentrations showing average values (black line) and 7-day smoothing (red dashed line); (upper middle) cumulative annual pollen totals; and (upper right) normalized cumulative sums used for phenological thresholding. The bottom row illustrates inter-annual trends over the 23-year period (2002-2024) for (lower left) season start day (2.5% threshold), (lower middle) season end day (97.5% threshold), and (lower right) the annual pollen integral (APIn). Linear regression lines and coefficients of determination (R^2) highlight a shift toward an earlier and more intense pollen season.

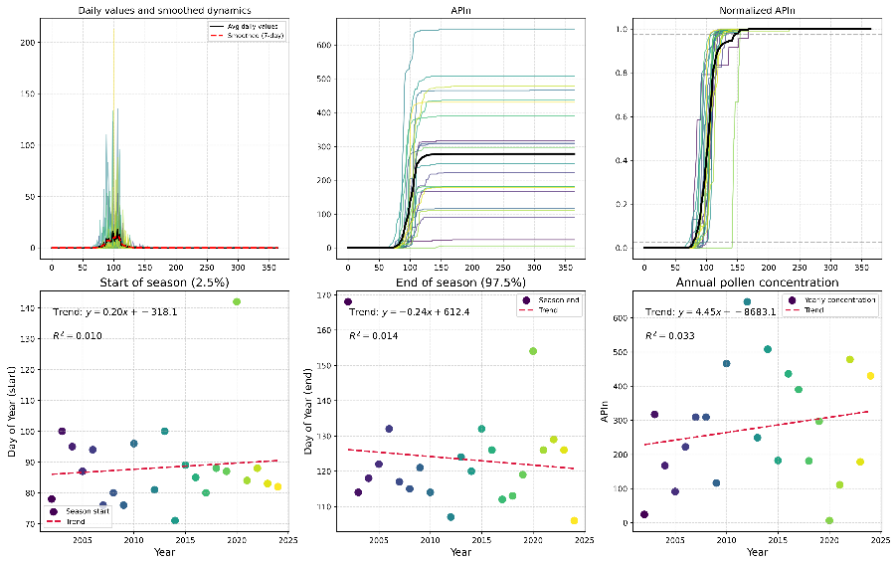

Figure S12d: Example of the pollen season analysis pipeline applied to *Betula* spp. (birch) in Primorje. The top row presents the seasonal dynamics and data normalization: (upper left) daily pollen concentrations showing average values (black line) and 7-day smoothing (red dashed line); (upper middle) cumulative annual pollen totals; and (upper right) normalized cumulative sums used for phenological thresholding. The bottom row illustrates inter-annual trends over the 23-year period (2002-2024) for (lower left) season start day (2.5% threshold), (lower middle) season end day (97.5% threshold), and (lower right) the annual pollen integral (APIn). Linear regression lines and coefficients of determination (R^2) highlight a shift toward an earlier and more intense pollen season.

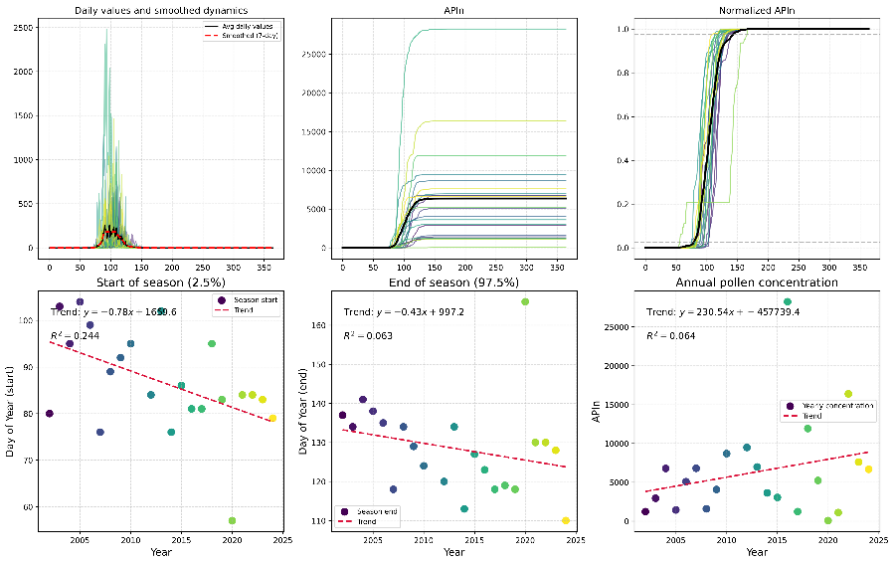

Figure S12e: Example of the pollen season analysis pipeline applied to *Carpinus* spp./*Ostrya* spp. (hornbeam/hop-hornbeam) in Primorje. The top row presents the seasonal dynamics and data normalization: (upper left) daily pollen concentrations showing average values (black line) and 7-day smoothing (red dashed line); (upper middle) cumulative annual pollen totals; and (upper right) normalized cumulative sums used for phenological thresholding. The bottom row illustrates inter-annual trends over the 23-year period (2002-2024) for (lower left) season start day (2.5% threshold), (lower middle) season end day (97.5% threshold), and (lower right) the annual pollen integral (APIn). Linear regression lines and coefficients of determination (R^2) highlight a shift toward an earlier and more intense pollen season.

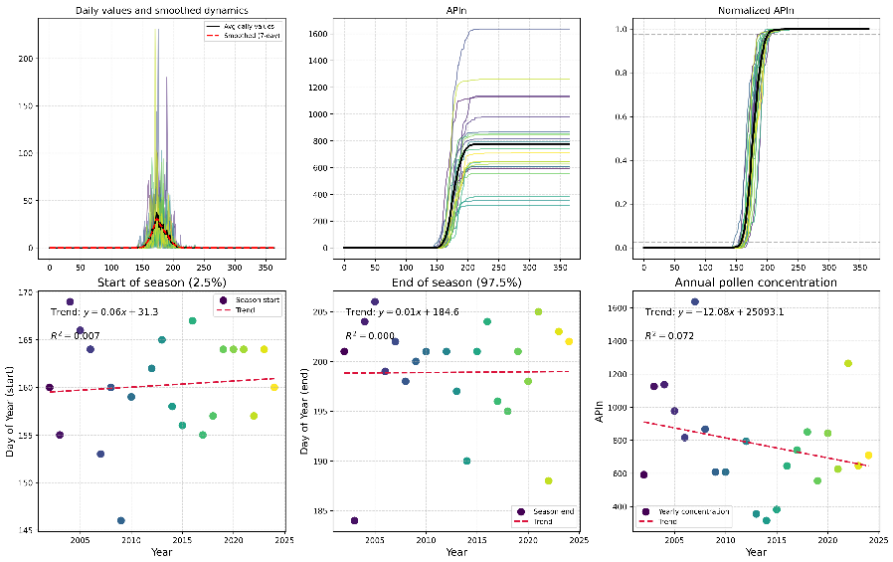

Figure S12f: Example of the pollen season analysis pipeline applied to *Castanea* sp. (sweet chestnut) in Primorje. The top row presents the seasonal dynamics and data normalization: (upper left) daily pollen concentrations showing average values (black line) and 7-day smoothing (red dashed line); (upper middle) cumulative annual pollen totals; and (upper right) normalized cumulative sums used for phenological thresholding. The bottom row illustrates inter-annual trends over the 23-year period (2002-2024) for (lower left) season start day (2.5% threshold), (lower middle) season end day (97.5% threshold), and (lower right) the annual pollen integral (APIn). Linear regression lines and coefficients of determination (R^2) highlight a shift toward an earlier and more intense pollen season.

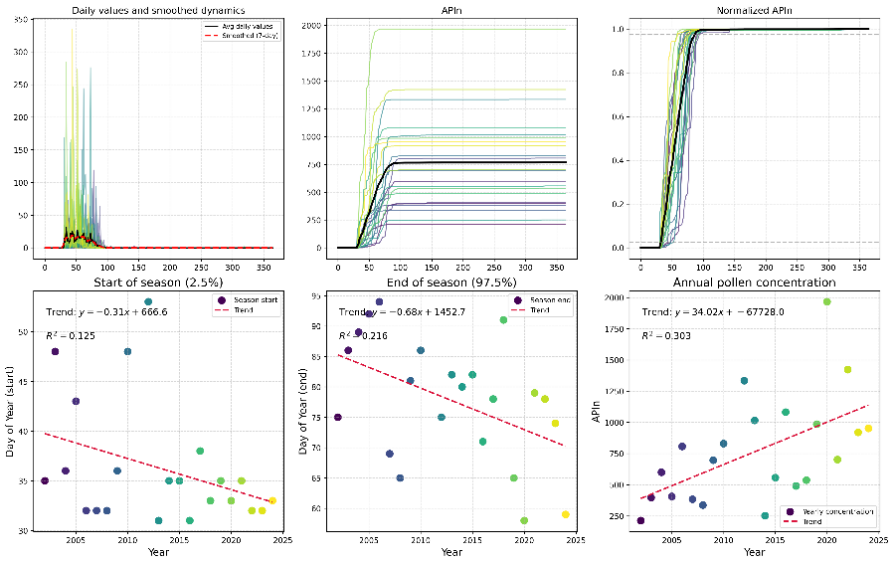

Figure S12g: Example of the pollen season analysis pipeline applied to *Corylus* sp. (hazel) in Primorje. The top row presents the seasonal dynamics and data normalization: (upper left) daily pollen concentrations showing average values (black line) and 7-day smoothing (red dashed line); (upper middle) cumulative annual pollen totals; and (upper right) normalized cumulative sums used for phenological thresholding. The bottom row illustrates inter-annual trends over the 23-year period (2002-2024) for (lower left) season start day (2.5% threshold), (lower middle) season end day (97.5% threshold), and (lower right) the annual pollen integral (APIn). Linear regression lines and coefficients of determination (R^2) highlight a shift toward an earlier and more intense pollen season.

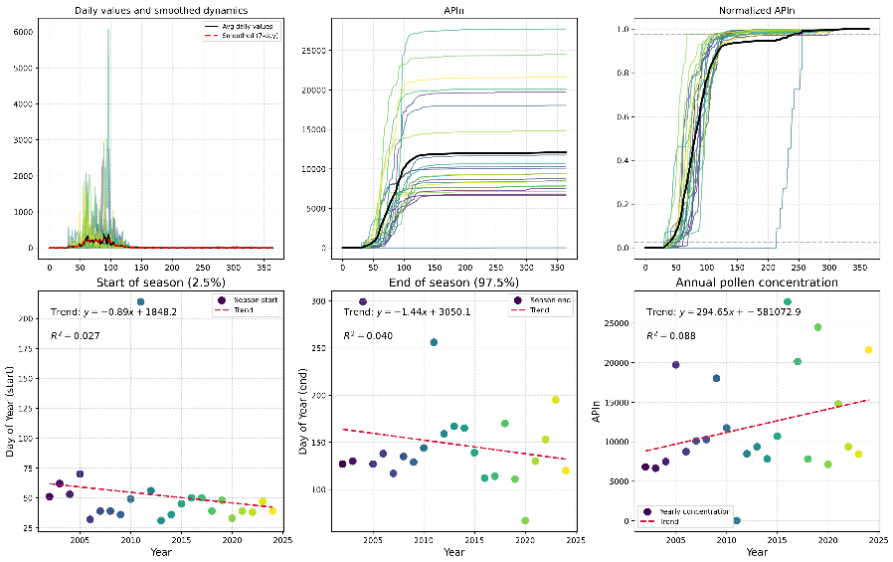

Figure S12h: Example of the pollen season analysis pipeline applied to Cupressaceae/Taxaceae (cypress/yew) in Primorje. The top row presents the seasonal dynamics and data normalization: (upper left) daily pollen concentrations showing average values (black line) and 7-day smoothing (red dashed line); (upper middle) cumulative annual pollen totals; and (upper right) normalized cumulative sums used for phenological thresholding. The bottom row illustrates inter-annual trends over the 23-year period (2002-2024) for (lower left) season start day (2.5% threshold), (lower middle) season end day (97.5% threshold), and (lower right) the annual pollen integral (APIn). Linear regression lines and coefficients of determination (R^2) highlight a shift toward an earlier and more intense pollen season.

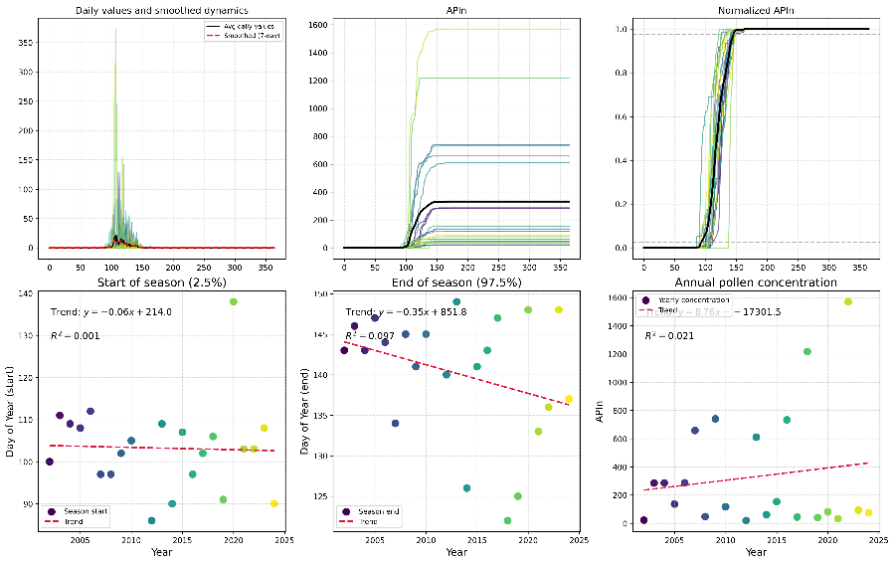

Figure S12i: Example of the pollen season analysis pipeline applied to *Fagus* sp. (beech) in Primorje. The top row presents the seasonal dynamics and data normalization: (upper left) daily pollen concentrations showing average values (black line) and 7-day smoothing (red dashed line); (upper middle) cumulative annual pollen totals; and (upper right) normalized cumulative sums used for phenological thresholding. The bottom row illustrates inter-annual trends over the 23-year period (2002-2024) for (lower left) season start day (2.5% threshold), (lower middle) season end day (97.5% threshold), and (lower right) the annual pollen integral (APIn). Linear regression lines and coefficients of determination (R^2) highlight a shift toward an earlier and more intense pollen season.

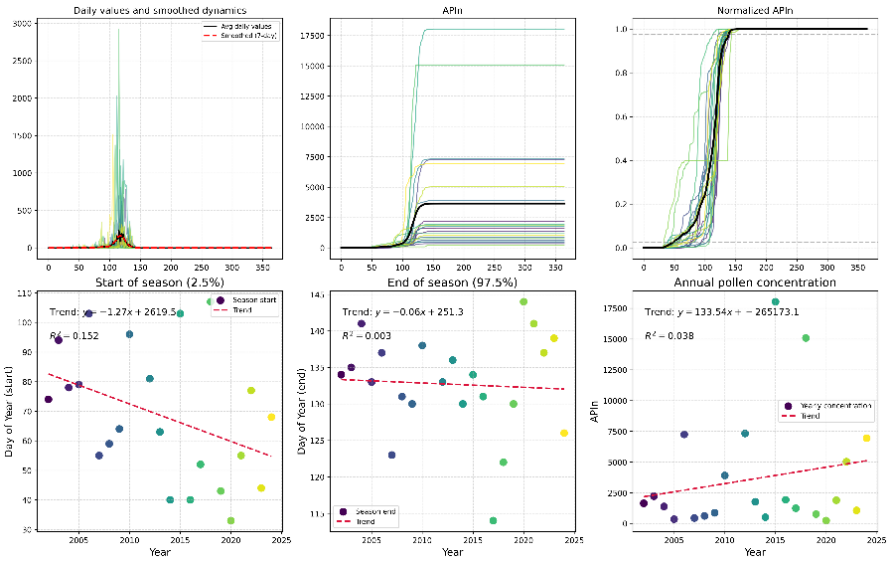

Figure S12j: Example of the pollen season analysis pipeline applied to *Fraxinus* spp. (ash) in Primorje. The top row presents the seasonal dynamics and data normalization: (upper left) daily pollen concentrations showing average values (black line) and 7-day smoothing (red dashed line); (upper middle) cumulative annual pollen totals; and (upper right) normalized cumulative sums used for phenological thresholding. The bottom row illustrates inter-annual trends over the 23-year period (2002-2024) for (lower left) season start day (2.5% threshold), (lower middle) season end day (97.5% threshold), and (lower right) the annual pollen integral (APIn). Linear regression lines and coefficients of determination (R^2) highlight a shift toward an earlier and more intense pollen season.

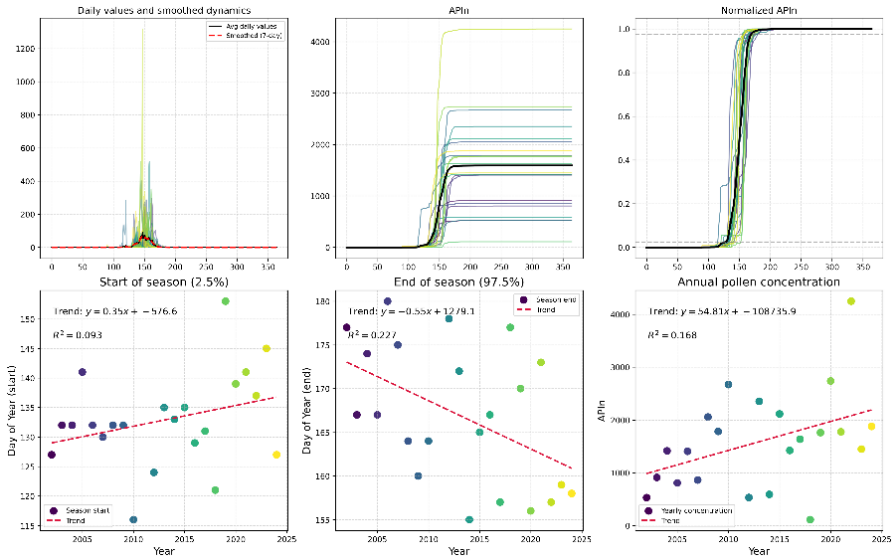

Figure S12k: Example of the pollen season analysis pipeline applied to *Olea* sp. (olive) in Primorje. The top row presents the seasonal dynamics and data normalization: (upper left) daily pollen concentrations showing average values (black line) and 7-day smoothing (red dashed line); (upper middle) cumulative annual pollen totals; and (upper right) normalized cumulative sums used for phenological thresholding. The bottom row illustrates inter-annual trends over the 23-year period (2002-2024) for (lower left) season start day (2.5% threshold), (lower middle) season end day (97.5% threshold), and (lower right) the annual pollen integral (APIn). Linear regression lines and coefficients of determination (R^2) highlight a shift toward an earlier and more intense pollen season.

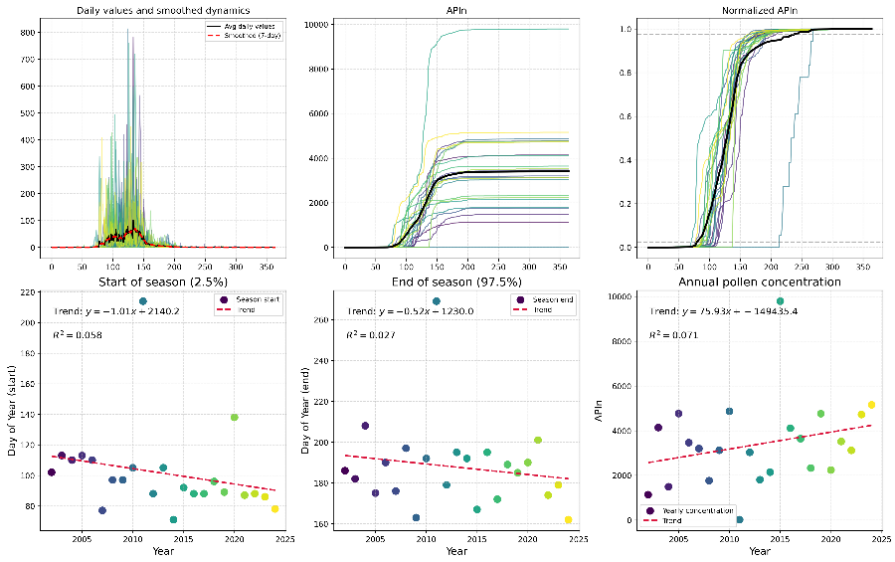

Figure S12l: Example of the pollen season analysis pipeline applied to *Pinus* spp. (pine) in Primorje. The top row presents the seasonal dynamics and data normalization: (upper left) daily pollen concentrations showing average values (black line) and 7-day smoothing (red dashed line); (upper middle) cumulative annual pollen totals; and (upper right) normalized cumulative sums used for phenological thresholding. The bottom row illustrates inter-annual trends over the 23-year period (2002-2024) for (lower left) season start day (2.5% threshold), (lower middle) season end day (97.5% threshold), and (lower right) the annual pollen integral (APIn). Linear regression lines and coefficients of determination (R^2) highlight a shift toward an earlier and more intense pollen season.

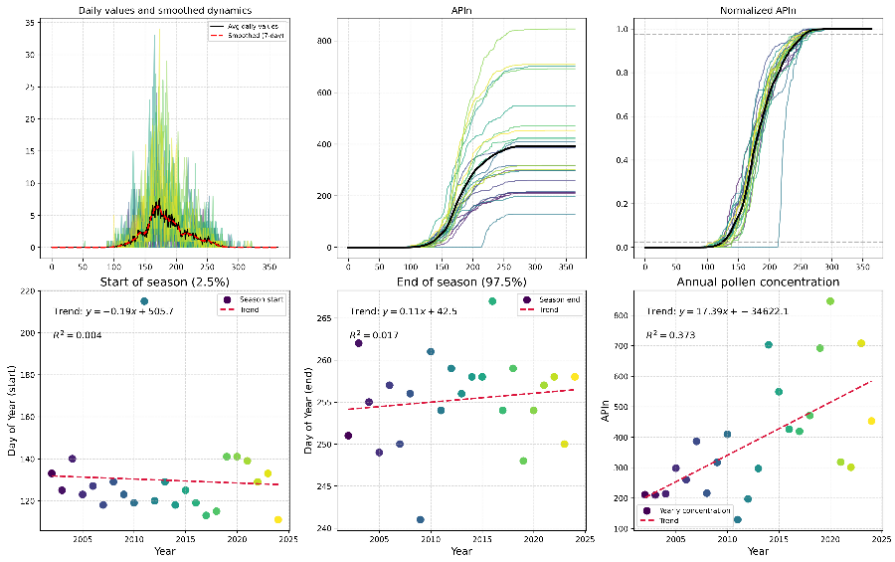

Figure S12m: Example of the pollen season analysis pipeline applied to *Plantago* spp. (plantain) in Primorje. The top row presents the seasonal dynamics and data normalization: (upper left) daily pollen concentrations showing average values (black line) and 7-day smoothing (red dashed line); (upper middle) cumulative annual pollen totals; and (upper right) normalized cumulative sums used for phenological thresholding. The bottom row illustrates inter-annual trends over the 23-year period (2002-2024) for (lower left) season start day (2.5% threshold), (lower middle) season end day (97.5% threshold), and (lower right) the annual pollen integral (APIn). Linear regression lines and coefficients of determination (R^2) highlight a shift toward an earlier and more intense pollen season.

Figure **S12**

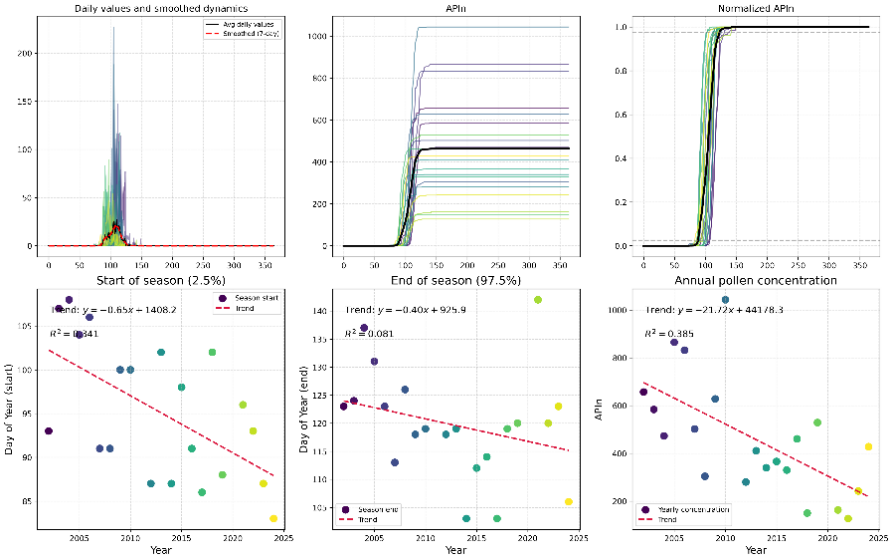

n: Example of the pollen season analysis pipeline applied to *Platanus* spp. (plane tree) in Primorje. The top row presents the seasonal dynamics and data normalization: (upper left) daily pollen concentrations showing average values (black line) and 7-day smoothing (red dashed line); (upper middle) cumulative annual pollen totals; and (upper right) normalized cumulative sums used for phenological thresholding. The bottom row illustrates inter-annual trends over the 23-year period (2002-2024) for (lower left) season start day (2.5% threshold), (lower middle) season end day (97.5% threshold), and (lower right) the annual pollen integral (APIn). Linear regression lines and coefficients of determination (R^2) highlight a shift toward an earlier and more intense pollen season.

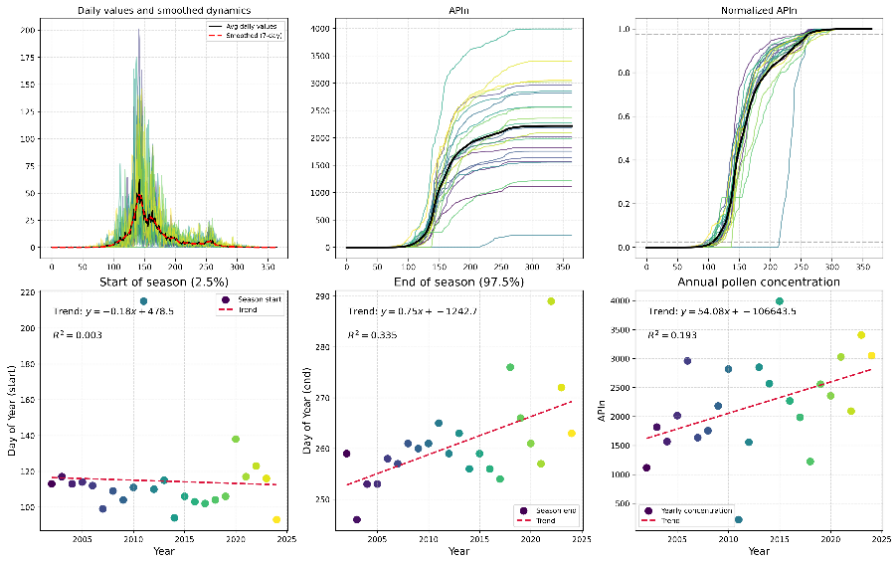

Figure S12o: Example of the pollen season analysis pipeline applied to Poaceae (grasses) in Primorje. The top row presents the seasonal dynamics and data normalization: (upper left) daily pollen concentrations showing average values (black line) and 7-day smoothing (red dashed line); (upper middle) cumulative annual pollen totals; and (upper right) normalized cumulative sums used for phenological thresholding. The bottom row illustrates inter-annual trends over the 23-year period (2002-2024) for (lower left) season start day (2.5% threshold), (lower middle) season end day (97.5% threshold), and (lower right) the annual pollen integral (APIn). Linear regression lines and coefficients of determination (R^2) highlight a shift toward an earlier and more intense pollen season.

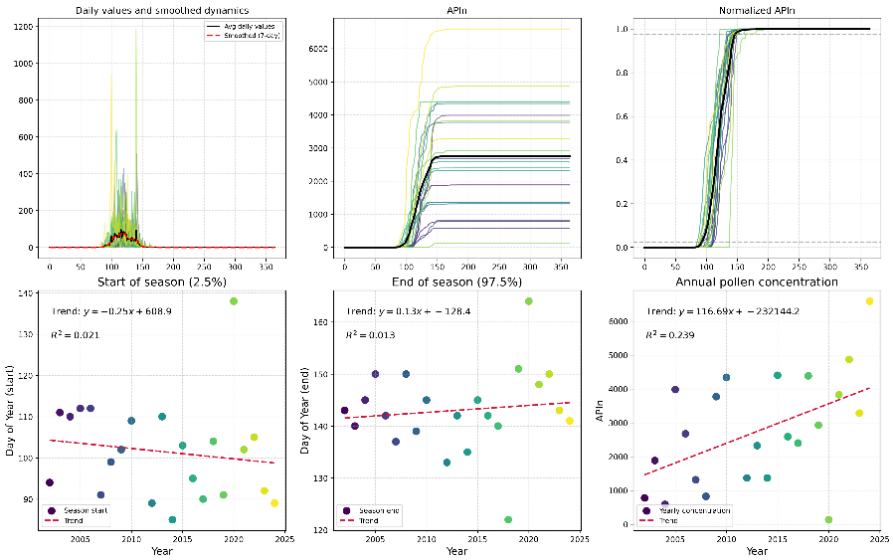

Figure S12p: Example of the pollen season analysis pipeline applied to *Quercus* spp. (oak) in Primorje. The top row presents the seasonal dynamics and data normalization: (upper left) daily pollen concentrations showing average values (black line) and 7-day smoothing (red dashed line); (upper middle) cumulative annual pollen totals; and (upper right) normalized cumulative sums used for phenological thresholding. The bottom row illustrates inter-annual trends over the 23-year period (2002-2024) for (lower left) season start day (2.5% threshold), (lower middle) season end day (97.5% threshold), and (lower right) the annual pollen integral (APIn). Linear regression lines and coefficients of determination (R^2) highlight a shift toward an earlier and more intense pollen season.

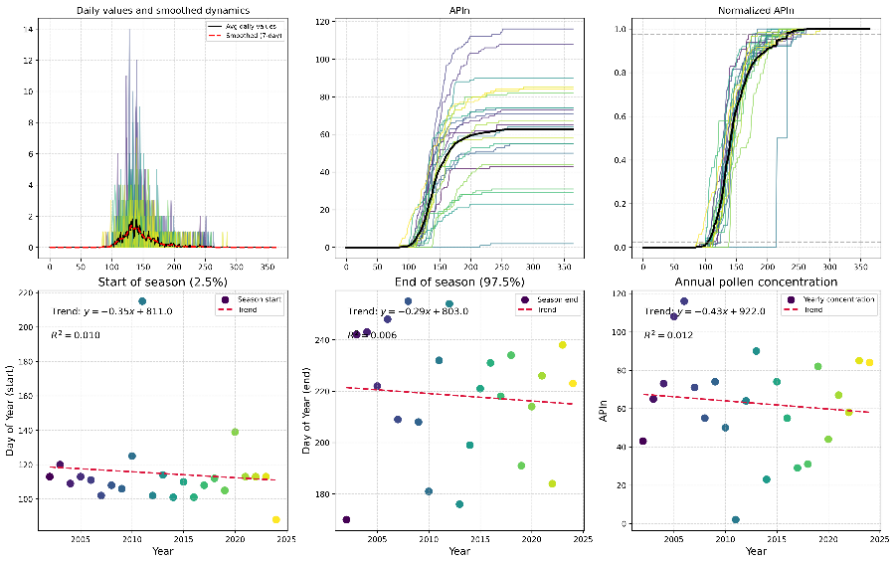

Figure S12q: Example of the pollen season analysis pipeline applied to *Rumex* spp. (dock) in Primorje. The top row presents the seasonal dynamics and data normalization: (upper left) daily pollen concentrations showing average values (black line) and 7-day smoothing (red dashed line); (upper middle) cumulative annual pollen totals; and (upper right) normalized cumulative sums used for phenological thresholding. The bottom row illustrates inter-annual trends over the 23-year period (2002-2024) for (lower left) season start day (2.5% threshold), (lower middle) season end day (97.5% threshold), and (lower right) the annual pollen integral (APIn). Linear regression lines and coefficients of determination (R^2) highlight a shift toward an earlier and more intense pollen season.

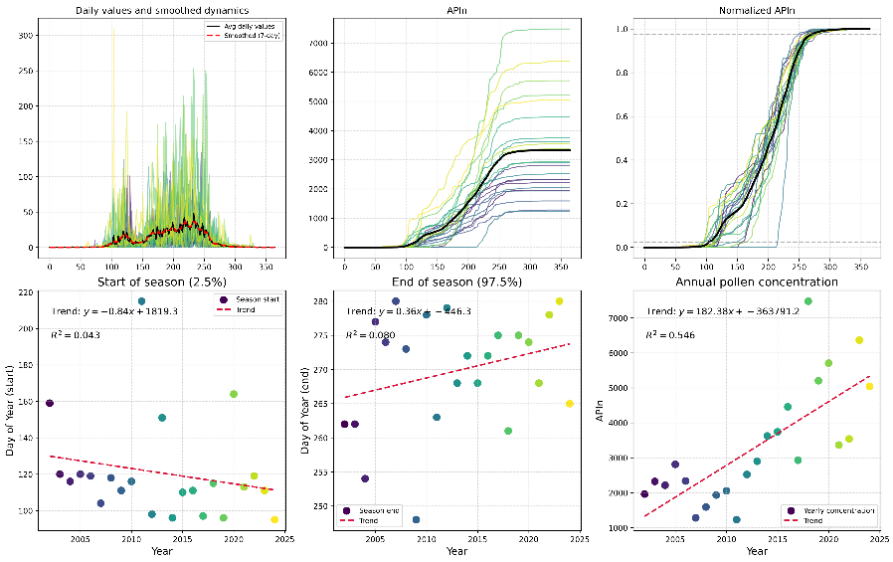

Figure S12r: Example of the pollen season analysis pipeline applied to Urticaceae (nettle) in Primorje. The top row presents the seasonal dynamics and data normalization: (upper left) daily pollen concentrations showing average values (black line) and 7-day smoothing (red dashed line); (upper middle) cumulative annual pollen totals; and (upper right) normalized cumulative sums used for phenological thresholding. The bottom row illustrates inter-annual trends over the 23-year period (2002-2024) for (lower left) season start day (2.5% threshold), (lower middle) season end day (97.5% threshold), and (lower right) the annual pollen integral (APIn). Linear regression lines and coefficients of determination (R^2) highlight a shift toward an earlier and more intense pollen season.

Cross-Regional Correlation Analysis

This section contains correlation analyses between different regions, showing relationships in pollen patterns across Ljubljana, Maribor, and Primorje.

Regional Correlation Results

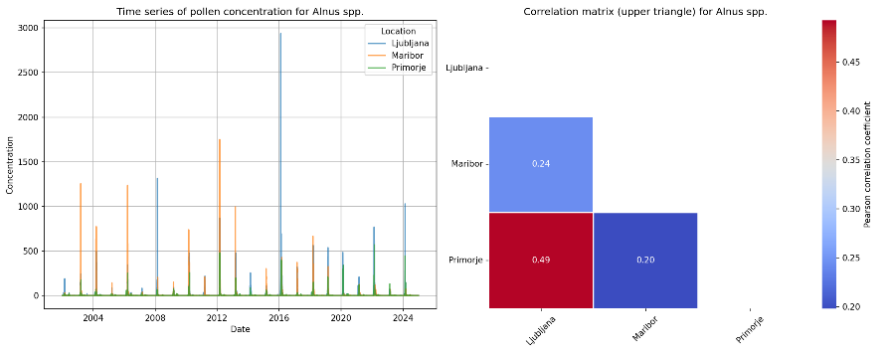

Figure S13a: Regional comparison of *Alnus spp.* (alder) pollen dynamics in Slovenia. (Left) Time series of daily pollen concentrations at three monitoring sites (Ljubljana, Maribor, Primorje) spanning 2002-2024. (Right) Correlation matrix showing inter-site relationships, with moderate to strong positive correlations indicating partially synchronized pollen seasons across locations, while regional differences in peak timing and intensity reflect local environmental conditions.

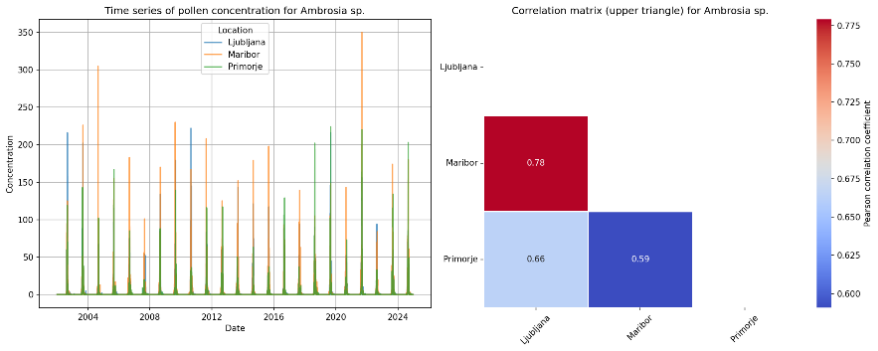

Figure S13b: Regional comparison of *Ambrosia* sp. (ragweed) pollen dynamics in Slovenia. (Left) Time series of daily pollen concentrations at three monitoring sites (Ljubljana, Maribor, Primorje) spanning 2002-2024. (Right) Correlation matrix showing inter-site relationships, with moderate to strong positive correlations indicating partially synchronized pollen seasons across locations, while regional differences in peak timing and intensity reflect local environmental conditions.

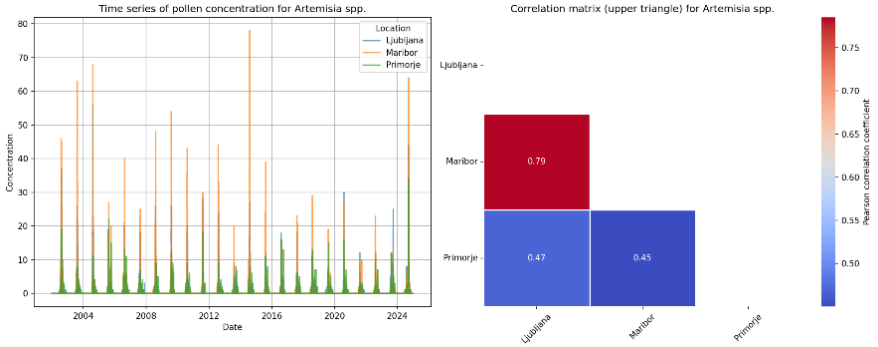

Figure S13c: Regional comparison of *Artemisia* spp. (mugwort) pollen dynamics in Slovenia. (Left) Time series of daily pollen concentrations at three monitoring sites (Ljubljana, Maribor, Primorje) spanning 2002-2024. (Right) Correlation matrix showing inter-site relationships, with moderate to strong positive correlations indicating partially synchronized pollen seasons across locations, while regional differences in peak timing and intensity reflect local environmental conditions.

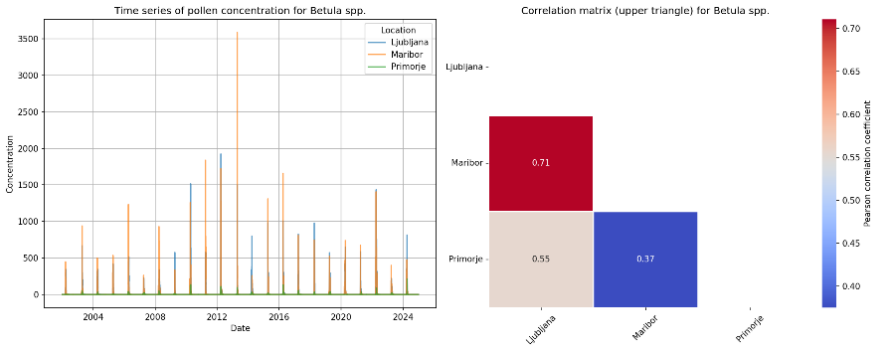

Figure S13d: Regional comparison of *Betula* spp. (birch) pollen dynamics in Slovenia. (Left) Time series of daily pollen concentrations at three monitoring sites (Ljubljana, Maribor, Primorje) spanning 2002-2024. (Right) Correlation matrix showing inter-site relationships, with moderate to strong positive correlations indicating partially synchronized pollen seasons across locations, while regional differences in peak timing and intensity reflect local environmental conditions.

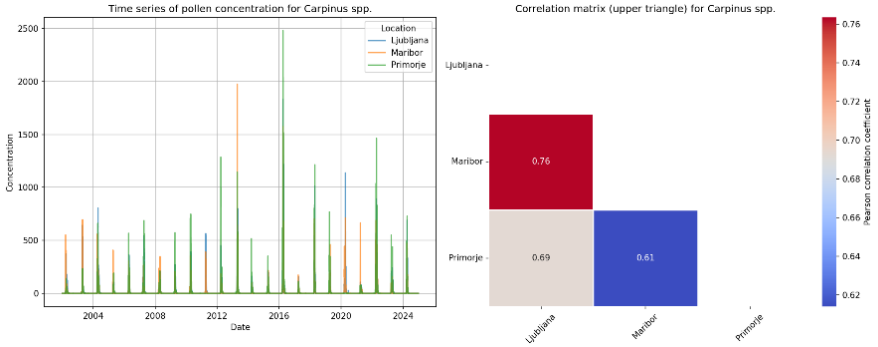

Figure S13e: Regional comparison of *Carpinus* spp./*Ostrya* spp. (hornbeam/hop-hornbeam) pollen dynamics in Slovenia. (Left) Time series of daily pollen concentrations at three monitoring sites (Ljubljana, Maribor, Primorje) spanning 2002-2024. (Right) Correlation matrix showing inter-site relationships, with moderate to strong positive correlations indicating partially synchronized pollen seasons across locations, while regional differences in peak timing and intensity reflect local environmental conditions.

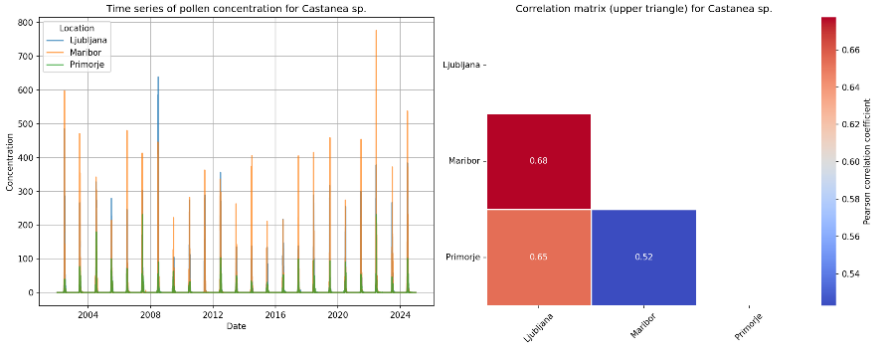

Figure S13f: Regional comparison of *Castanea* sp. (sweet chestnut) pollen dynamics in Slovenia. (Left) Time series of daily pollen concentrations at three monitoring sites (Ljubljana, Maribor, Primorje) spanning 2002-2024. (Right) Correlation matrix showing inter-site relationships, with moderate to strong positive correlations indicating partially synchronized pollen seasons across locations, while regional differences in peak timing and intensity reflect local environmental conditions.

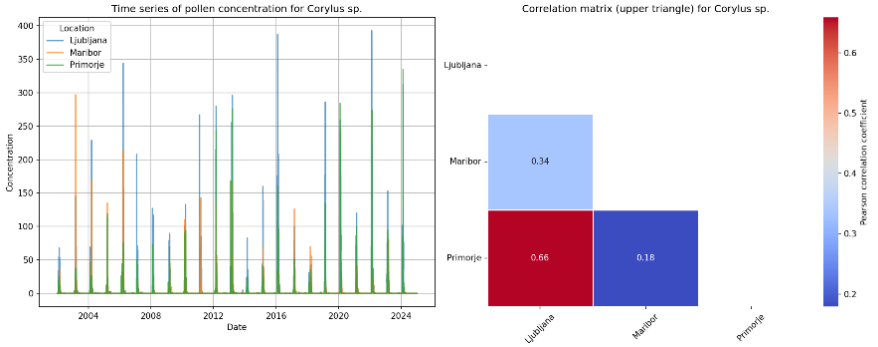

Figure S13g: Regional comparison of *Corylus* sp. (hazel) pollen dynamics in Slovenia. (Left) Time series of daily pollen concentrations at three monitoring sites (Ljubljana, Maribor, Primorje) spanning 2002-2024. (Right) Correlation matrix showing inter-site relationships, with moderate to strong positive correlations indicating partially synchronized pollen seasons across locations, while regional differences in peak timing and intensity reflect local environmental conditions.

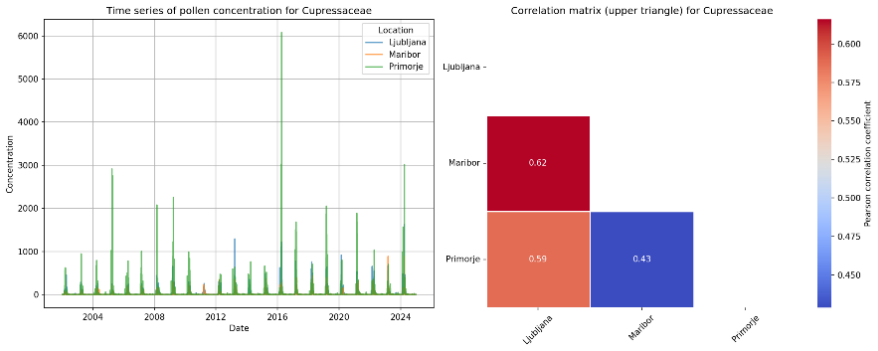

Figure S13h: Regional comparison of Cupressaceae/Taxaceae (cypress/yew) pollen dynamics in Slovenia. (Left) Time series of daily pollen concentrations at three monitoring sites (Ljubljana, Maribor, Primorje) spanning 2002-2024. (Right) Correlation matrix showing inter-site relationships, with moderate to strong positive correlations indicating partially synchronized pollen seasons across locations, while regional differences in peak timing and intensity reflect local environmental conditions.

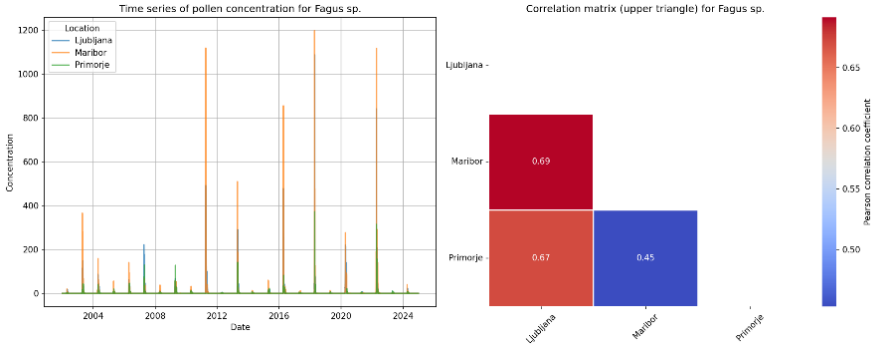

Figure S13i: Regional comparison of *Fagus* sp. (beech) pollen dynamics in Slovenia. (Left) Time series of daily pollen concentrations at three monitoring sites (Ljubljana, Maribor, Primorje) spanning 2002-2024. (Right) Correlation matrix showing inter-site relationships, with moderate to strong positive correlations indicating partially synchronized pollen seasons across locations, while regional differences in peak timing and intensity reflect local environmental conditions.

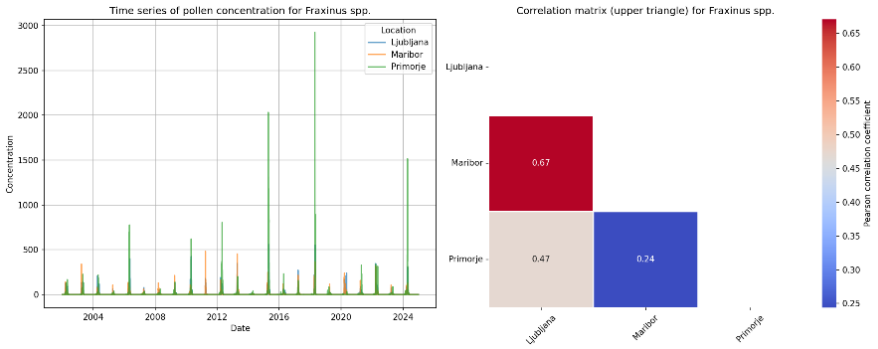

Figure S13j: Regional comparison of *Fraxinus* spp. (ash) pollen dynamics in Slovenia. (Left) Time series of daily pollen concentrations at three monitoring sites (Ljubljana, Maribor, Primorje) spanning 2002-2024. (Right) Correlation matrix showing inter-site relationships, with moderate to strong positive correlations indicating partially synchronized pollen seasons across locations, while regional differences in peak timing and intensity reflect local environmental conditions.

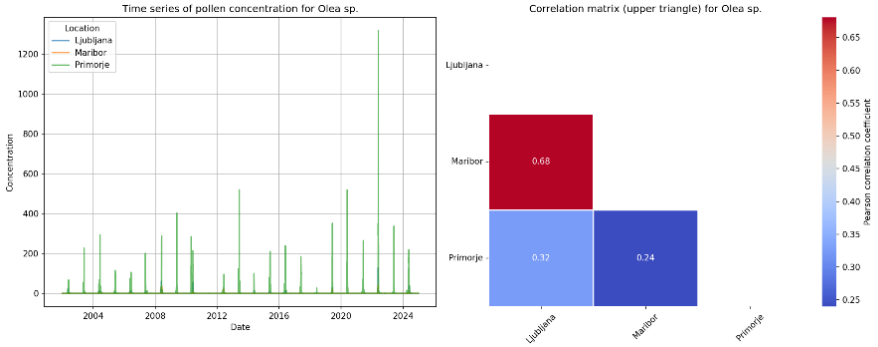

Figure S13k: Regional comparison of *Olea* sp. (olive) pollen dynamics in Slovenia. (Left) Time series of daily pollen concentrations at three monitoring sites (Ljubljana, Maribor, Primorje) spanning 2002-2024. (Right) Correlation matrix showing inter-site relationships, with moderate to strong positive correlations indicating partially synchronized pollen seasons across locations, while regional differences in peak timing and intensity reflect local environmental conditions.

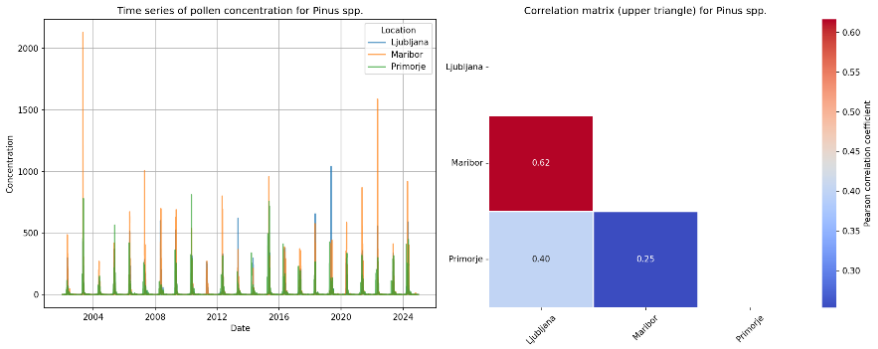

Figure S13l: Regional comparison of *Pinus* spp. (pine) pollen dynamics in Slovenia. (Left) Time series of daily pollen concentrations at three monitoring sites (Ljubljana, Maribor, Primorje) spanning 2002-2024. (Right) Correlation matrix showing inter-site relationships, with moderate to strong positive correlations indicating partially synchronized pollen seasons across locations, while regional differences in peak timing and intensity reflect local environmental conditions.

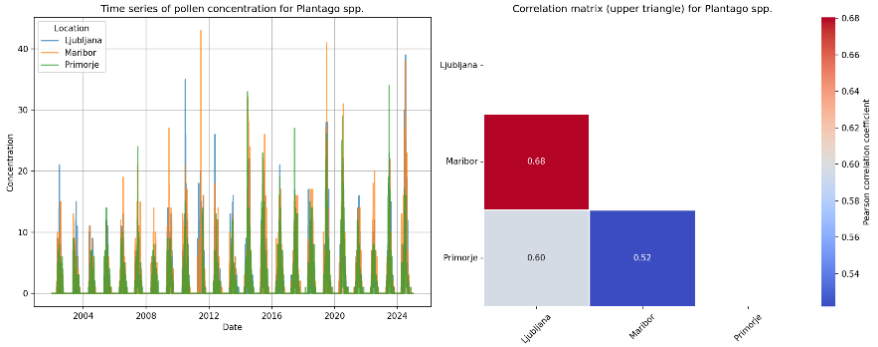

Figure S13m: Regional comparison of *Plantago* spp. (plantain) pollen dynamics in Slovenia. (Left) Time series of daily pollen concentrations at three monitoring sites (Ljubljana, Maribor, Primorje) spanning 2002-2024. (Right) Correlation matrix showing inter-site relationships, with moderate to strong positive correlations indicating partially synchronized pollen seasons across locations, while regional differences in peak timing and intensity reflect local environmental conditions.

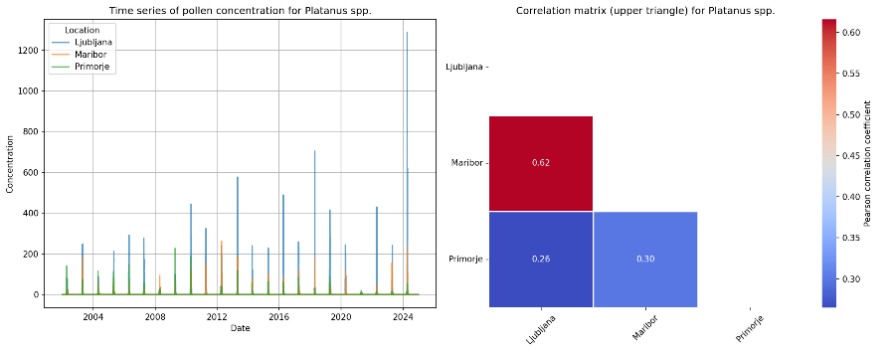

Figure S13n: Regional comparison of *Platanus* spp. (plane tree) pollen dynamics in Slovenia. (Left) Time series of daily pollen concentrations at three monitoring sites (Ljubljana, Maribor, Primorje) spanning 2002-2024. (Right) Correlation matrix showing inter-site relationships, with moderate to strong positive correlations indicating partially synchronized pollen seasons across locations, while regional differences in peak timing and intensity reflect local environmental conditions.

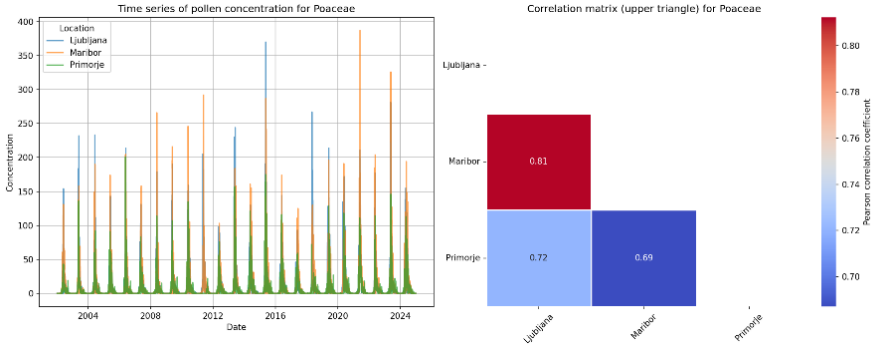

Figure S13o: Regional comparison of Poaceae *(*grasses) pollen dynamics in Slovenia. (Left) Time series of daily pollen concentrations at three monitoring sites (Ljubljana, Maribor, Primorje) spanning 2002-2024. (Right) Correlation matrix showing inter-site relationships, with moderate to strong positive correlations indicating partially synchronized pollen seasons across locations, while regional differences in peak timing and intensity reflect local environmental conditions.

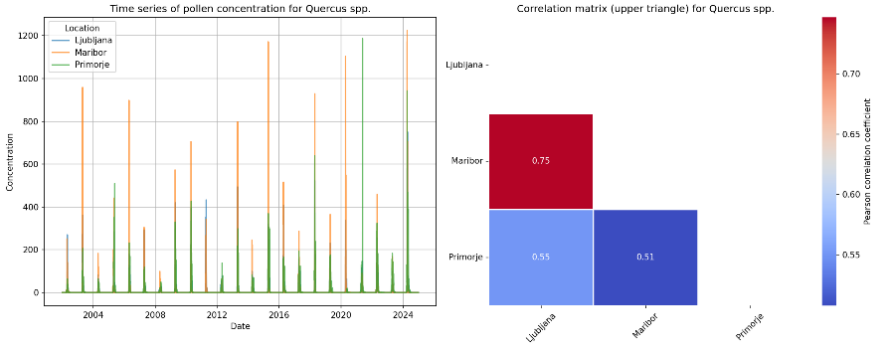

Figure S13p: Regional comparison of *Quercus* spp. (oak) pollen dynamics in Slovenia. (Left) Time series of daily pollen concentrations at three monitoring sites (Ljubljana, Maribor, Primorje) spanning 2002-2024. (Right) Correlation matrix showing inter-site relationships, with moderate to strong positive correlations indicating partially synchronized pollen seasons across locations, while regional differences in peak timing and intensity reflect local environmental conditions.

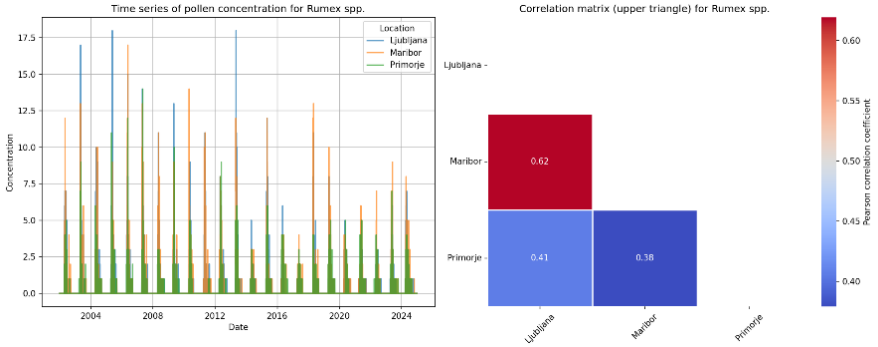

Figure S13q: Regional comparison of *Rumex* spp. (dock) pollen dynamics in Slovenia. (Left) Time series of daily pollen concentrations at three monitoring sites (Ljubljana, Maribor, Primorje) spanning 2002-2024. (Right) Correlation matrix showing inter-site relationships, with moderate to strong positive correlations indicating partially synchronized pollen seasons across locations, while regional differences in peak timing and intensity reflect local environmental conditions.

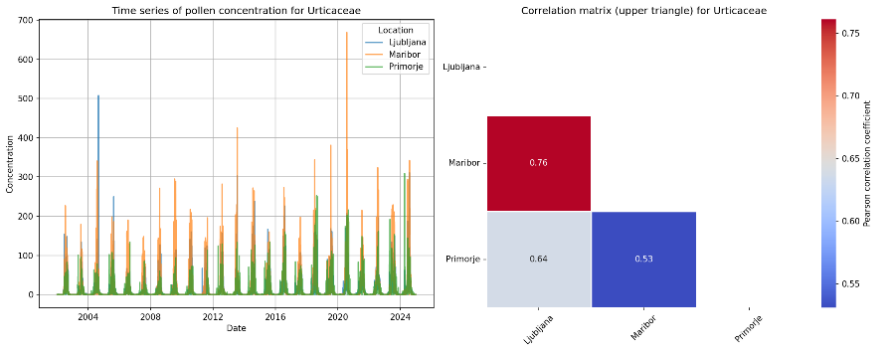

Figure S13r: Regional comparison of Urticaceae (nettle) pollen dynamics in Slovenia. (Left) Time series of daily pollen concentrations at three monitoring sites (Ljubljana, Maribor, Primorje) spanning 2002-2024. (Right) Correlation matrix showing inter-site relationships, with moderate to strong positive correlations indicating partially synchronized pollen seasons across locations, while regional differences in peak timing and intensity reflect local environmental conditions.